EIC Detector R&D Progress Report

The EIC Tracking and PID Consortium
(eRD6 Consortium)

June 26, 2020

The eRD6 Consortium

Project ID: eRD6

Project Name: Tracking & PID detector R&D towards an EIC detector

Period Reported: from January 2020 to June 2020

Brookhaven National Lab (BNL): Craig Woody

Florida Institute of Technology (Fl. Tech): Marcus Hohlmann

INFN Trieste: Silvia Dalla Torre

CEA Saclay: Francesco Bossù, Maxence Vandenbroucke

Stony Brook University (SBU): Klaus Dehmelt, Thomas Hemmick

Temple University (TU): Matt Posik, Bernd Surrow

University of Virginia (UVa): Kondo Gnanvo, Nilanga Liyanage

Yale University: Richard Majka*, Nikolai Smirnov

Project Members:

BNL: B. Azmoun, A. Kiselev, J. Kuczewski, M. L. Purschke, C. Woody

Fl. Tech: J. Chesslo, J. Collins, M. Hohlmann, M. Lavinsky, B. Steffen

INFN Trieste: S. Dalla Torre, S. Levorato, F. Tessarotto

CEA Saclay: Stephane Aune, Francesco Bossù, Maxime Defurne, Aude Glaenzer, Qinhua Huang, Maxence Revolle, Franck Sabatié, Maxence Vandenbroucke

SBU: K. Dehmelt, A. Deshpande. P. Garg, T. K. Hemmick, A. Kulkarni, S. Park, C.L. Perez, V. Zakharov, A. Zhang

TU: N. Lukow, M. Posik, A. Quintero, B. Surrow

UVa: Minh Dao, K. Gnanvo, N. Liyanage

Yale University: R. Majka*, N. Smirnov

* deceased

Contact Person: Kondo Gnanvo; kgnanvo@virginia.edu

Contents

1 Introduction

1.1 Brief overview of eRD6 project histories

The overall main focus of the R&D conducted by the eRD6 consortium has been the development of micro-pattern gas detectors (MPGD's) such as GEM, THGEMs, Micromegas, μRWELL, for tracking and particle identification at a future EIC. While each institution has been focusing on specific technical aspects of the R&D, much synergy has been produced with several collaborative efforts created over the years. For central tracking, BNL, Stony Brook and Yale have been mounting a long-term investigation of GEM-based TPCs readout structure, while Florida Tech, Temple U., and UVa have closely collaborated on the design, production, and testing of large GEM detector for the forward tracker. They jointly designed GEM foils for the EIC forward GEM Tracker prototypes and they have conducted combined beam tests at Fermilab. The latter three groups more recently teamed up to study the potential for a fast central tracker based on μRWELL detector technology and are collaborating to build the first fully operational cylindrical μRWELL prototype ever built worldwide. The team at CEA Saclay also recently join eRD6 consortium to explore the possibility for Micromegas technology to be proposed as a main EIC central tracker. The PID effort within eRD6 is spearheaded and is continued by Stony Brook U. and INFN Trieste with a focus on MPGD-based photon detection and the development of optical elements for high momentum RICH applications. The entire group meets bi-weekly to discuss progress and problems and to coordinate efforts. In addition, a smaller subgroup meets regularly on simulation efforts.

1.2 eRD6 Contribution to EIC Yellow Report Effort

The eRD6 consortium is playing an important role in the elaboration of the EIC Yellow Report (YR) document with contributions to several YR Working Groups (WGs), in particular Tracking and PID WGs. The developments performed within eRD6 activities are injected as input material in the relevant WGs, often accompanied by a dedicated effort to shape the information in a form adequate for the Yellow Report initiative. This core effort is accompanied by some specific personal contributions by eRD6 members:

- **Silvia Dalla Torre from INFN Trieste** is one of the conveners of the YR Detector Working Group (YR-DWG) overlooking the broad discussions related to the various EIC detector options under consideration including the detector integration and the complementarity aspects of different detector options. Her role as convener is complemented by her contribution to the discussions in WGs: PID, DAQ and electronics, integration and central magnet.
- **Kondo Gnanvo from University of Virginia** is one of conveners of the Tracking WG, one of the subgroups of the YR-DWG. He is specifically looking at all the aspect of gaseous detectors options including MPGDs technologies for EIC central tracking detector which include both the barrel and both end cap trackers.
- **Thomas Hemmick from Stony Brook University** is one of the conveners of the PID WG, one of the subgroups of the YR-DWG. He is dedicating specific effort to the comparative analysis of the several technologies proposed in order to perform PID from the low momenta ($\sim$1 GeV/c) up to the high ones ($\sim$50 GeV/c).
- **Alexander Kiselev from Brookhaven National** Lab is one of the conveners of the integration and central magnet WG, one of the subgroups of the YR-DWG. Among other efforts, he has built a software tool for fast modelling and generation of EIC Central Detector templates.
- **Matt Posik from Temple University** is the liaison between eRD6 groups and the YRWGs including physics working group (PWG), detector working group (DWG) and software group (SWG).

2 Barrel Tracker with TPC

2.1 What was planned for this period?

2.1.1 TPC studies at Brookhaven National Lab and Yale Univ.

The goals for this funding cycle are listed below:

1. Design and procure a new TPC zigzag PCB and start studying the prototype detector response using the new laser system. The plan was to initially outfit the prototype with GEMs, then with Micromegas and μRWELL if time permits. We expected to qualify these measurements by comparing them with results from cosmic tracks. Finally, we expected to read out the prototype with DREAM and SAMPA FEE.
2. Use the new high intensity, narrow beam x-ray source to measure the response of new zigzag patterns for potential use in the TPC. Time permitting, the new TPC readout boards equipped with a 4-GEM, Micromegas and μRWELL will all initially be scanned with the x-ray scanner prior to being installed in the TPC prototype. We planned to use the DREAM and possibly SAMPA FEE to read out the detectors under test here as well.
3. Characterization of potential TPC avalanche stages with various gas mixtures, performed at Yale.

2.1.2 TPC studies at Stony Brook

Planned efforts at SBU were to continue the investigation of IBF blocking structures to be used in an MPGD-based readout structure for a TPC. In particular, the concept of a passive gating grid is in the focus of our investigations.

2.2 What was achieved?

2.2.1 TPC studies at Brookhaven National Lab and Yale Univ.

Results from new x-ray scanner setup: The assembly of our high flux, narrow beam x-ray source is now complete and we have started doing preliminary measurements with it. The source consists of a 50W x-ray source equipped with a copper target and produces a spectrum of x-rays highly peaked at 8keV, with a relatively narrow cone of illumination (25deg. full angle). The output flux is collimated down to a beam spot of about 25μm by 1mm, with a divergence of about 0.25mrad along the smaller dimension. The raw collimated output produces rates well above 50kHz, as detected with a standard GEM detector. As shown in Fig. 1, the source is attached to a XY-stage capable of incrementing the position of the source by as little as 6.35μm per motor step along the coordinate readout of a given detector under test.

To characterize the x-ray beam, we exposed a standard GEM with COMPASS readout (with 400μm pitched anode strips) to the x-ray source and scanned across at least 5 pitch cycles along the sensitive coordinate. The collimator was also rotationally oriented such that the 25μ width of the beam spot probed the sensitive coordinate. By examining some basic performance plots for this detector, we hope to better understand the diagnostic capabilities of this unique x-ray source.

Fig. 2 shows the preliminary results of the scan, including the scatter of the residuals and centroid per event versus the motor position. Though there appears to be a good correlation between the motor position and the measured centroid position, the slight deviation from a unity slope may be explained by a slight angular offset of the PCB coordinate system with respect to the direction of the motor travel. It was found that this

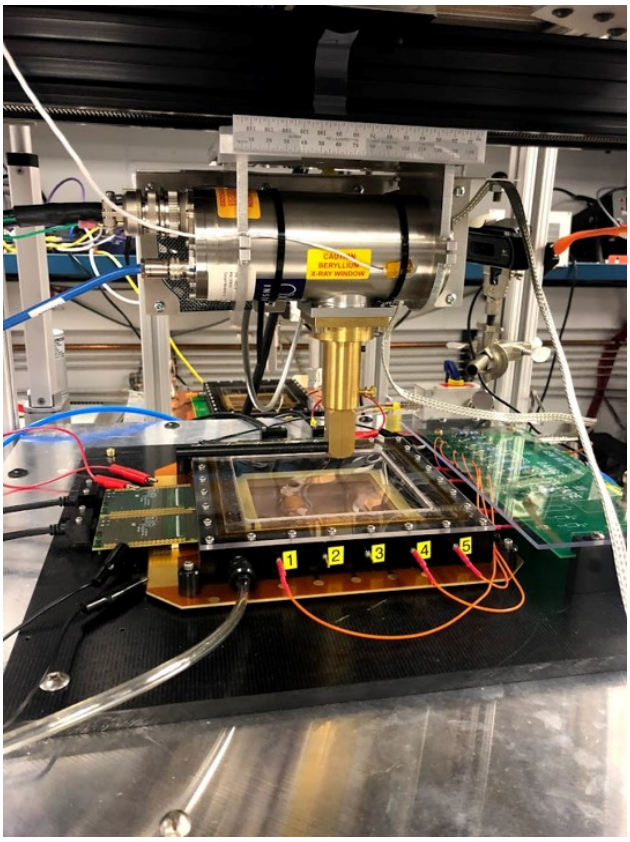

Figure 1: Picture of the assembled x-ray scanner setup with a GEM detector with COMPASS readout being scanned.

angle was approximately 1.4 degrees, which represents a systematic error that is easily accounted for and has a negligible impact on the effective beam width of 25 μm along the sensitive coordinate. Also apparent in the scatter plots is a slight kink in the trend, which may reveal a slight imperfection in the anode geometry (which requires further confirmation). In addition, the deviations from a perfectly linear response of the readout is revealed as a repeated diagonal micro-structure in the residual scatter plot. Such feature-finding capabilities make this setup a valuable tool for inspecting the performance of readout PCBs under test.

Fig. 3 shows the position resolution and the cluster size as a function of the motor position. While the position resolution is more or less flat, it fluctuates between 80μm and about 100μm, where the larger values tend to coincide with the kink in the trend discussed earlier, which may be a further indication of some issue with the readout board in this location. The cluster size oscillates between 9,10, and 11 pad clusters, which depends on whether the incident charge impacts the center of a single pad or in between two pads. In any case, the cluster size seems quite high, which may be partially due to bipolar signals induced on neighboring pads from cross talk. However, it was found that increasing the zero suppression threshold by a factor of two results in a slight deterioration of the resolution, which implies the eliminated signals were not from cross-talk.

The left plots in Fig. 4 show the cumulative residual distribution from the position scan, along with the resulting cluster size distribution. These results are compared to the residual and cluster size distributions measured with a very similar detector in a particle beam. For the x-ray scan the reference point for the residual is taken as the motor position whereas the reference during the beam test was provided by a high resolution silicon telescope (as described in earlier reports). In this case, the residual distribution is substantially narrower than what is measured using the x-ray source (i.e., 55μm versus 77μm). The mean cluster size for the x-ray data is also markedly larger than for the beam data (i.e., 9.9 pads versus 7.4 pads),

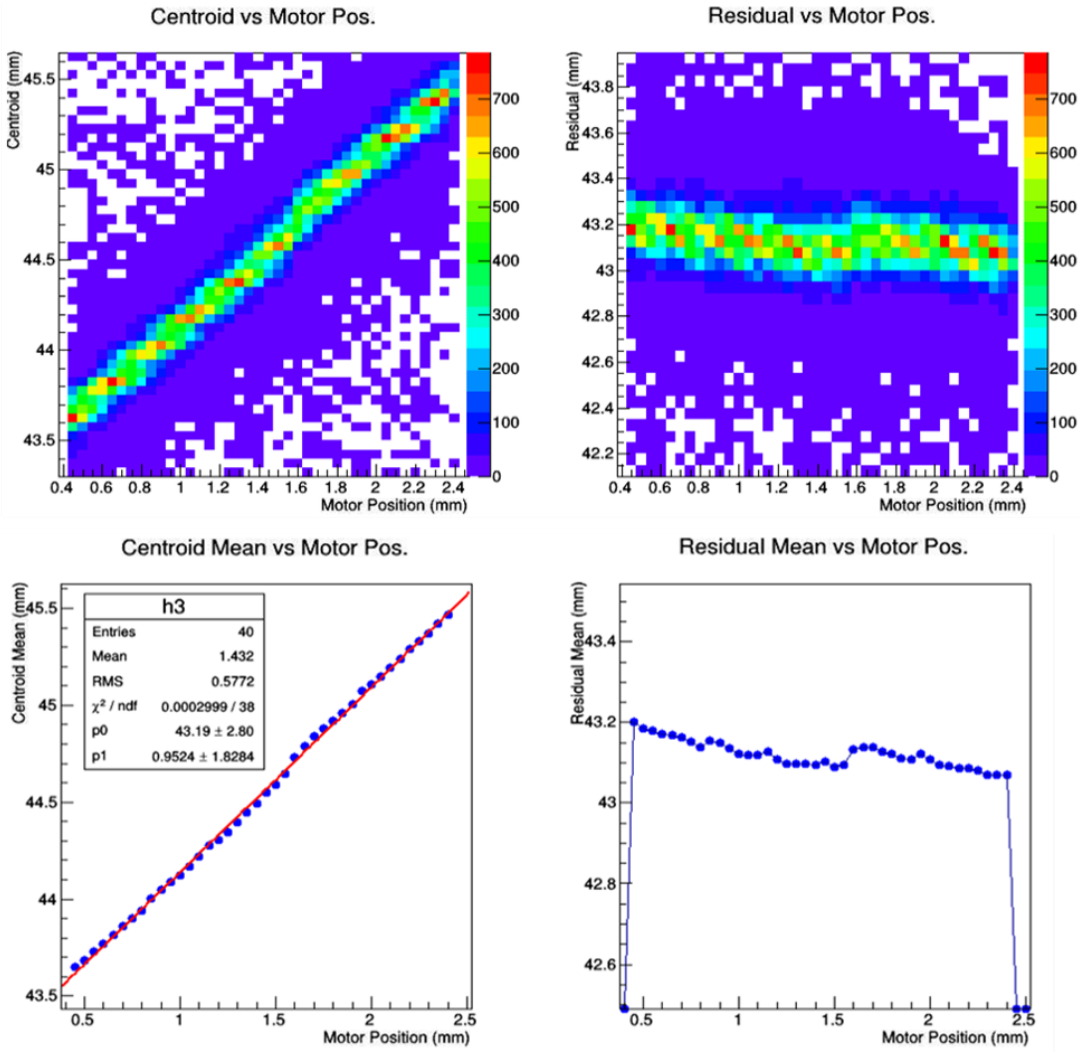

Figure 2: The two top panels show the scatter plots of the centroid and residual per event respectively, and the bottom plots show the respective means of the scatter data versus the motor position.

though the beam data has a long tail. One leading hypothesis is that the photoelectron range from x-ray conversions in the working gas is large enough that it contributes significantly to the primary cluster width. As a result, the measured resolution is comprised of the intrinsic resolution of the readout (whcih is primarily a function of the anode shape and pitch), the width of the incident charge cloud, and the uncertainty in the conversion point within the gas. The last component is constrained by the fine collimation of the x-ray beam and is therefore negligible, however the absorption of an 8keV x-ray produces both 3keV and 5keV photoelectrons, the latter of which has a range approaching 300μm in argon.Taking the quadrature difference in the resolutions measured with the x-ray source and the particle beam, the contribution from the resulting charge cloud on the measured resolution is about 55μm. The ability for the x-ray source to measure resolutions well below about 80μm therefore appears to be limited. (It should noted that these are only preliminary conclusions that could change upon further investigation into this matter.)

To recuperate this ability, it would be interesting to illuminate a Mn plate with the source flux in order to generate fluorescence photons characteristic of an Fe55 source (as we've already done with an older x-ray source). These photons are highly monochromatic and are peaked at 5.89keV and produce 3keV photoelectrons, with a substantially smaller electron range in argon (below 100μm). An alternative would be to illuminate a microscopic region of the GEM surface with a UV laser to liberate photoelectons, which

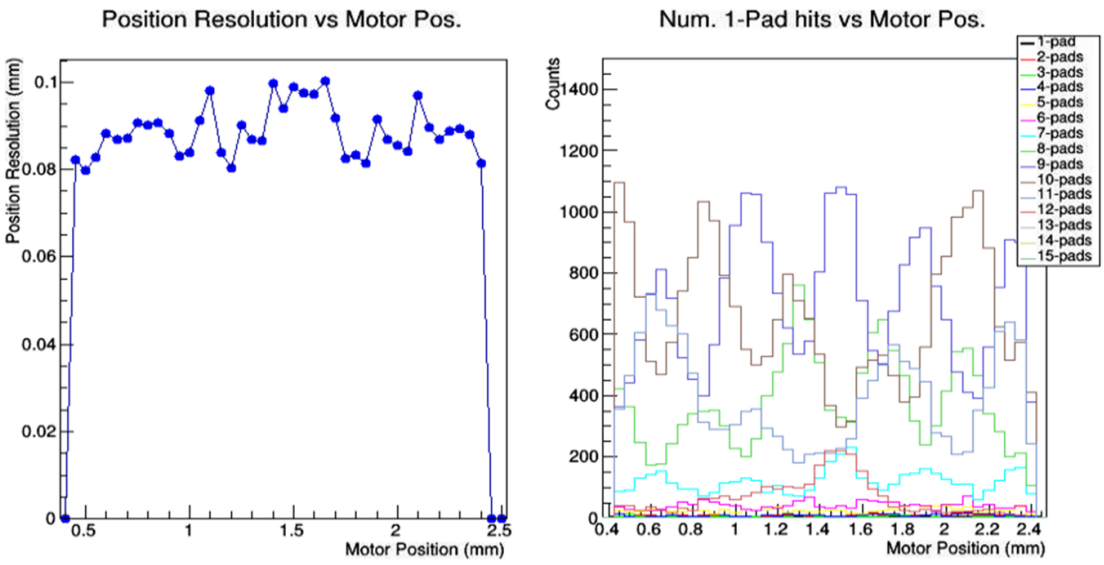

Figure 3: The position resolution versus the motor position and the cluster size trends versus motor position.

would also act as a high resolution reference point. This idea is discussed further in a later section.

Study of TPC gain element and gas mixture: A Time Projection Chamber (TPC) is on the list of options for barrel tracking & PID. It is well known that a TPC has low X0 with good charge particle track-finding, momentum reconstruction and dE/dx performance. The next step is to use a TPC as a high rate detector (with no gating grid), which is already in progress at ALICE. An EIC TPC would require a low number of pad rows; the only solution is to get the best possible precision for charge cluster position reconstruction. This means a low transverse diffusion gas mixture, and "modification" of readout pad structure (ZZ) and FEEs (timing & noise).

It was demonstrated that 150 μm space resolution for a 1 m drift TPC can be a reality (ILC, sPHENIX). However, the challenge is to guarantee that all known TPC distortions should be controlled or/and corrected with the same (or better) precision. The main distortion for a high rate TPC are Space Charge Distortions (SCD) due to slow drifting ions in the TPC volume. These distortions are a function of the interaction rate and background (primary ionization), gas gain, and ion backflow (IBF)/ion drift speed. (The last item is especially important for the high luminosity upgrades expected at the EIC.) For dE/dx measurements it is reasonable to increase the primary ionization and gain to get the best possible energy resolution for the readout.

In order to investigate the possible options for a future high rate TPC we have tested various gas gain structures and gas mixtures. Our goal was to focus on crucial TPC parameters: ion backflow, energy resolution (dE/dx), electron and ion drift speed, electron diffusion (in E- and B-fields), and stability. We concentrated on two options for the gain structure: 4 GEMs and MMG+2GEMs. As shown in Fig. 5, for the hybrid option we achieve simultaneously an ion back flow below 0.3% (with 10–15% uncertainty) and an energy resolution better than 12% (with 3–5% uncertainty) for 55Fe x-rays at a gain of ≈2000 in a variety of gas mixtures.

A MMG + 1-2 GEM setup in combination with CsI and Gas Cherenkov radiator is also an option that can be tested as possible PiD and PicoSecond (PS) fast detector. Measurements have been started to check the possibility to get a high Gas Gain in CF4 for MMG + GEM setup. Some preliminary results are shown in Fig. 6.

Newly published paper: "Design Studies of High Resolution Readout Planes using Zigzags with GEM Detectors",published in IEEE TNS (May 2020).

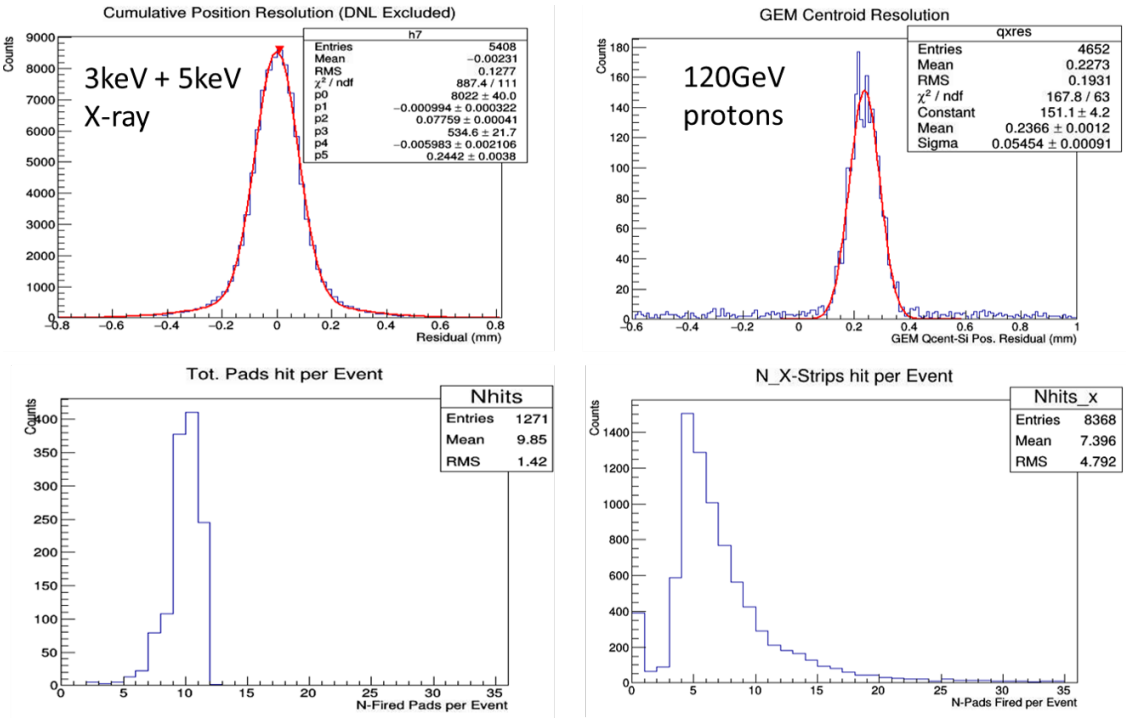

Figure 4: The left two panels show the cumulative residual distribution (top) and the cluster size distribution (bottom) for the x-ray scan. The right panels show the same plots for measurements made with a replica of this detector at a particle beam. The double Gaussian fit on the left takes into account a small background and reveals the position resolution as the sigma of the dominant Gaussian function ("p2").

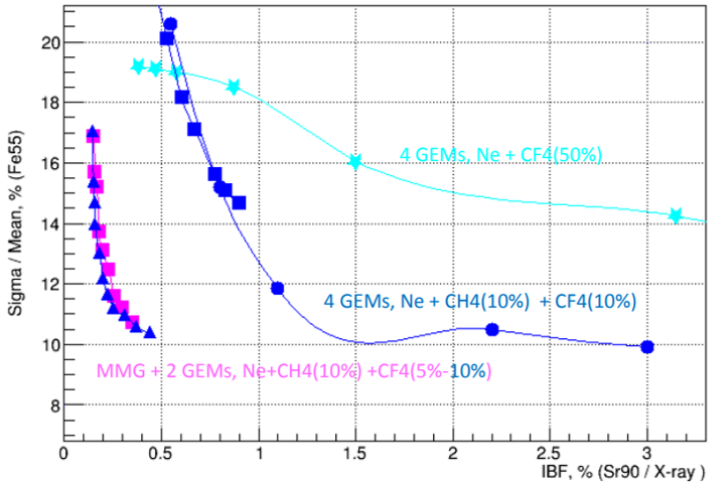

Figure 5: Energy resolution versus IBF for a MMG+2GEM hybrid detector filled with several different gas mixtures.

Update for mini-TPC prototype: Although we have not been able to conduct all the measurements originally planned using the mini-TPC prototype in the lab due to the pandemic, we did manage to make some progress on this front. We have completed the design of the new zigzag PCB for the prototype and have since received the fabricated PCB. The final drawing is shown in Fig. 7.

Additionally, we have prepped the TPC vessel to accept the new PCB. This includes the design of a new

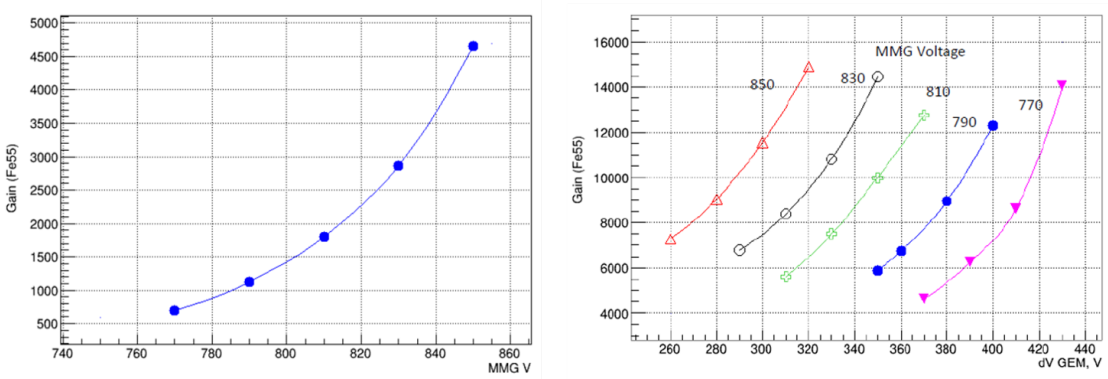

Figure 6: Left: Gain curve for MMG detector with CF4 working gas. Right: Gain curves for MMG+2GEM hybrid detector in CF4 (with 0.4kV/cm drift field and 1.2kV/cm extraction field).

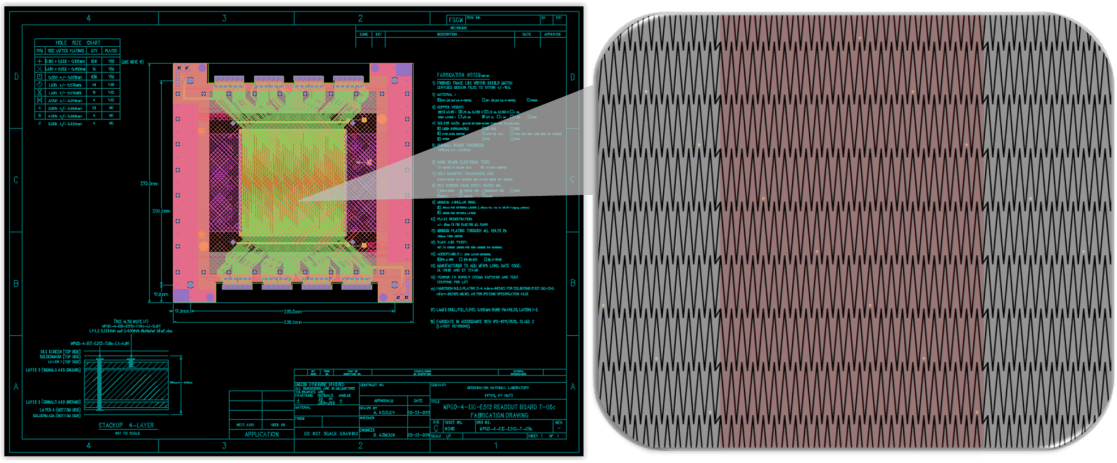

Figure 7: Engineering drawing of zigzag readout PCB for TPC prototype. The zigzag pattern consists of a pitch = 2mm, period = 0.5mm, stretch = 15%, and gap 50 microns. The inset picture of the zigzag pattern highlights a single pad row.

port to route diffuse UV laser light via a fiber optical cable to illuminate the inner surface of the field cage cathode (see Fig. 8). The surface is covered with an arrayed pattern of 1cm x 1mm rectangular Al strips which liberate electron clusters once illuminated, for the purpose of producing reference/calibration points for the TPC. This will provide an interesting tool to study the uniformity of the position resolution, gain, drift velocity, etc. The prototype will ultimately be equipped with two separate laser systems for the purpose of calibrating the detector and precisely measuring its performance: a straight line laser source for creating tracks (described in the previous report) and the new diffuse source for generating discrete clusters.

TPC readout options: We have made good progress regarding the analysis of beam test data conducted last spring to measure the position resolution of several MPGDs equipped with zigzag readouts. GEM, Micromegas, and μRWELL detectors, each in a planar configuration with a small drift gap were equipped with a readout PCB with an array of different zigzag shaped anode patterns. Fig. 9 illustrates each detector layout and includes a picture of the setup at the beam test. The objective was to find the readout pattern that resulted in the best performance (in terms of position and angular resolution) for each MPGD. Specifically, the optimal zigzag pattern is identified by observing which zigzag geometry produces a minimum in the resolution. The data collected here is relevant for our TPC R&D since it provides a baseline comparison of the various readout schemes that may considered for a TPC.

The results for these MPGDs is summarized in the plots in Fig. 10. These results are not exhaustive in the

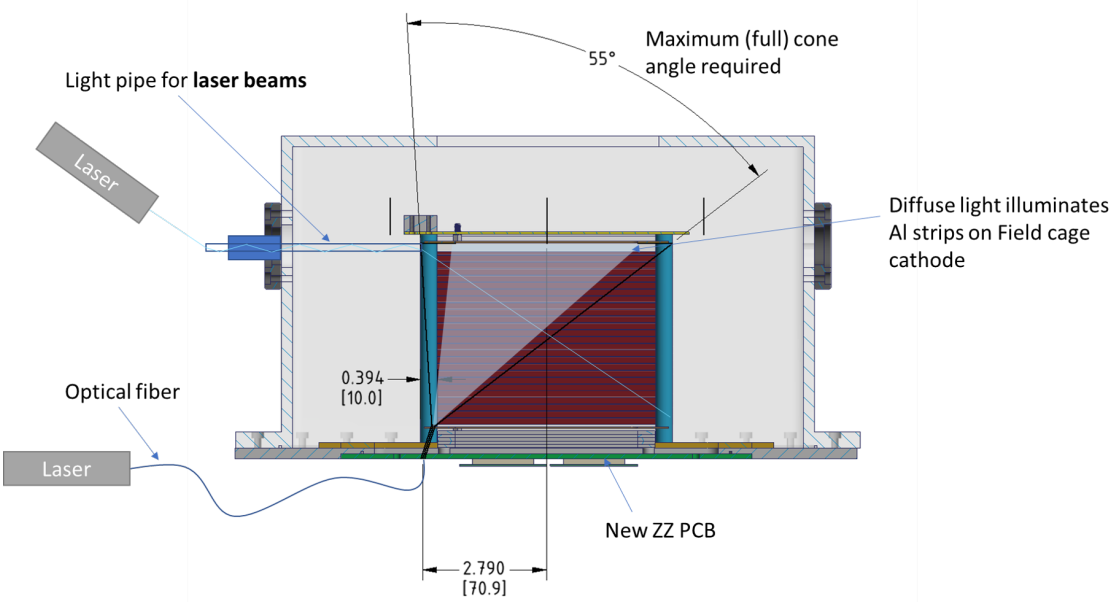

Figure 8: Model of the mini-TPC prototype illustrating the introduction of a laser beam into the TPC volume via a quartz bar and a diffuse source of laser light via a fiber optical cable for the purpose of illuminating an array of aluminum strips on the field cage cathode inner surface.

sense that the operating gas was not fully investigated yet, however there are already good indications for pairing each MPGD with an optimal zigzag pattern. It is still too early to choose the optimal anode pattern and MPGD combination, however we can at this point eliminate a substantial portion of this parameter space as a suitable option for the TPC.

2.2.2 TPC studies at Stony Brook

For ion back flow suppression in the TPC we have been performing static bipolar gating grid simulations for a large parameter space (wire diameter, pitch, potential across wires, various gas mixtures etc., see [1]). Based on the simulation inputs, we are planning to test the gating grid concept in a strong magnetic field at the Argonne National Laboratory facility, which provides an MRI magnet that can deliver fields up to B = 5 Tesla. In order to perform this test, we will have to include a wire plane on top of four GEM stack in the prototype setup.
Since it will not be convenient to open the TPC for swapping different configurations during the test, we have designed a PCB based pad plane to attach the wires and provide them with appropriate potentials via a routing scheme. Fig. 11, left, shows a schematic of the wire plane's active area matched to the as built GEM module design. Four different configurations (as shown in the color scheme) are implemented on the grid that can be tested simultaneously. It has to be noted that the sPHENIX TPC has its modules arranged in a polar co-ordinate system, which might pose a constraint for gating operation; the wires need to be parallel to each other for static gating operation. Therefore, we also want to investigate how much fanning out can be tolerated for such operation, along with different pitches for parallel wires in Cartesian coordinates.
Fig. 11, middle, shows a PCB design for wire plane in Eagle electronic design automation program which we have designed to couple with the TPC prototype.
One of the features of our designed board is the placement of connecting pads where the wires are soldered and glued (for mechanical strength). As can be seen in Fig. 11, right, the edge of such pads will serve for the purpose of alignment as $\sim 50\,\mu m$ wires are difficult to wind with precision.

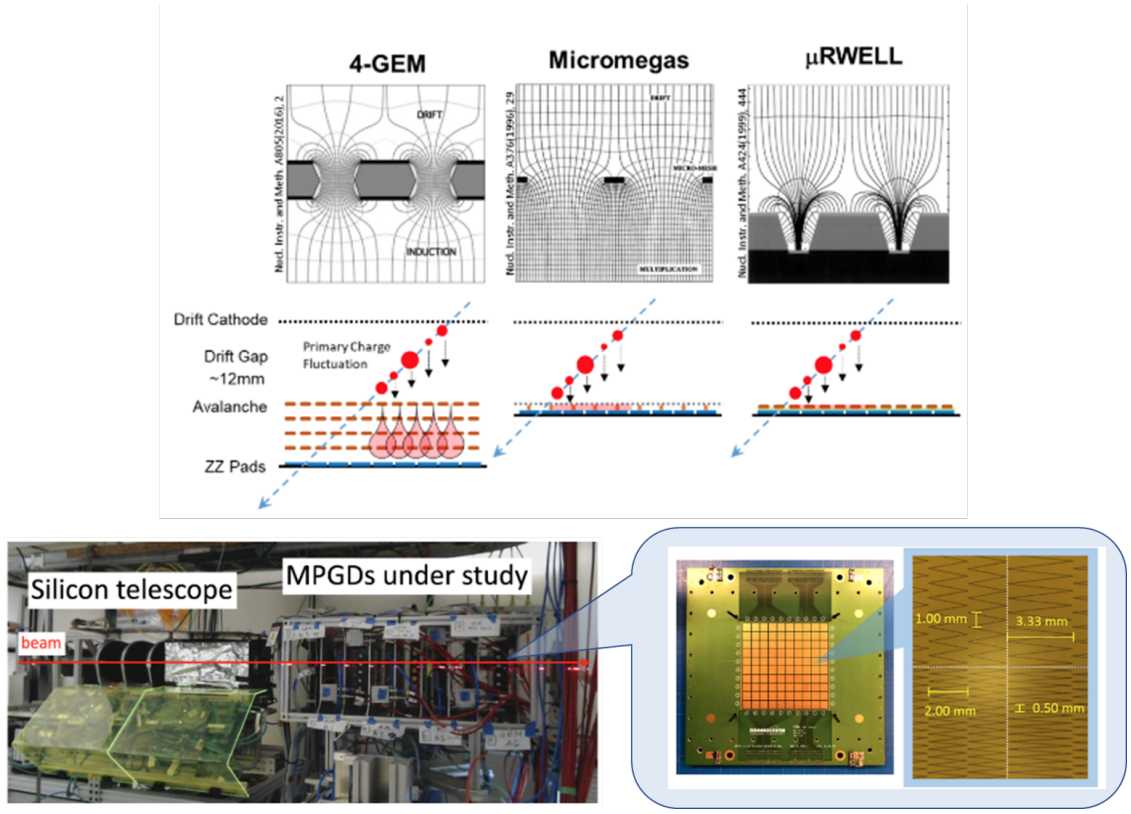

Figure 9: Top: the configuration for a GEM, Micromegas, and μRWELL planar detector measured at the Fermilab beam test in spring 2019 is shown here. Bottom: a picture of the multi-detector mount in the beam-line and a picture of one of the the readout PCBs is also shown. The readout PCB for each detector is comprised of an array of different zigzag patterns, separated by the dashed line in the bottom-right picture.

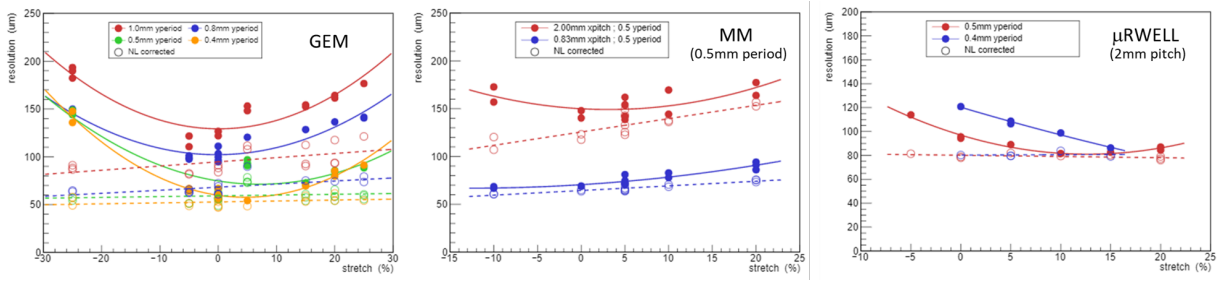

Figure 10: The position resolution versus the zigzag stretch parameter (defined as the fraction of a pitch cycle that neighboring pads overlap) for a GEM, Micromegas, and μRWELL planar detector.

2.3 What was not achieved, why not and what will be done to correct?

2.3.1 TPC studies at Brookhaven National Lab and Yale Univ.

All work conducted on site at Brookhaven Lab was effectively halted on March 20 due to the COVID-19 pandemic. This prevented us from performing the following planned measurements in the lab:

1. Characterization of the mini-TPC performance using the straight-line laser system
2. Characterization of Micromegas and μRWELL readouts

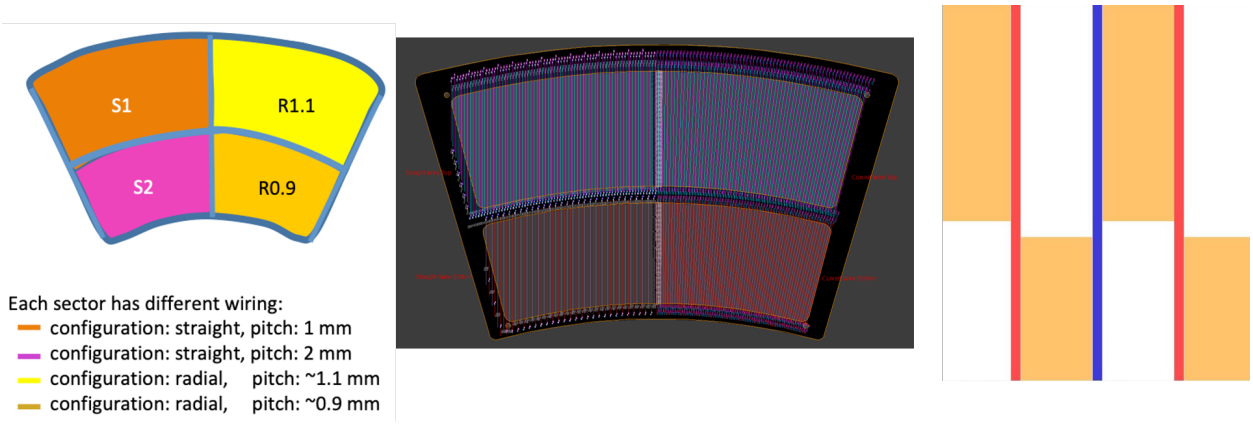

Figure 11: Left: Schematic of the wire plane active area. Middle: PCB for the mesh in the Eagle design automation program. Right: Zoom-in of the pad scheme.

3. Comparison to measurements with cosmic telescope
4. Baseline tests of readout detectors in x-ray scanner setup
5. We had planned to test a number of different readout options for various types of MPGDs in the test beam in the spring of this year as part of our LDRD on MPGDs that would have included a first iteration of readout boards specifically designed for our prototype TPC but these tests were cancelled due to COVID-19. We are now planning to do these tests in 2021.

2.3.2 TPC studies at Stony Brook

The technical implementation of a passive gating grid has yet to be performed. Due to the closure of the laboratory activities have stalled. The work on this project is ongoing. We are awaiting response from ANL when their operation will resume and this will allow us to plan for the tests with the magnet to be performed.

2.4 What is planned for the next funding cycle and beyond?

2.4.1 TPC studies at Brookhaven National Lab and Yale Univ.

A substantial portion of our planned activities for the next funding cycle will include work that was not completed as a result of the shutdown of the lab due to the pandemic. Our proposed R&D activity for the next funding cycle is as follows:

- Test and install new zigzag PCB onto TPC prototype and measure tracks produced by the laser (high statistics) and compare to cosmic tracks (low statistics). Time permitting, we would like to equip the TPC with a Micromegas and μRWELL avalanche stage to compare the performance, using both DREAM and SAMPA FEEs.
- Use the high intensity x-ray scanner to test each readout pattern + avalanche combination independent from the TPC field cage to provide a baseline comparison of each readout. These tests will likely be done with either DREAM or SAMPA FEEs. At some point next year we also plan to test several of these avalanche + readout schemes in a test beam, which we will start preparing for this year.
- It was determined that electron clusters resulting from x-ray conversions in the working gas of our detectors are large enough in size to significantly broaden residual distributions measured with our

narrow beam x-ray source, compared to what is measured with the same detectors in a high energy particle beam. Therefore, it would be highly beneficial to investigate ways of establishing a smaller reference point of charge for high resolution measurements in the lab. As a result, we plan to pursue the possibility of illuminating the top surface of GEM or μRWELL with a UV laser with a microscopic beam spot. A laser beam may be collimated with an aperture with a radius of tens of microns to liberate a similar sized cluster of electrons, which may potentially serve as an adequate reference for resolution measurements well below 100 microns. At the very least, this measurement could provide a means of accurately accounting for the excess broadening of residual distributions measured with the x-ray source.

- Finally, we propose to characterize various interesting TPC gas candidates by comparing the TPC performance with each gas. These studies may include gas gain measurements, attachment, drift velocity, charge spread measurements, and IBF measurements.
- We plan to design and test several new interleaved r/o anode designs intended for a photosensitive LAPPD detector.

2.4.2 TPC studies at Stony Brook

The implementation of a passive gating grid and its investigation at ANL is highest priority for the study of TPC optimization at SBU.

3 Full Barrel Tracker with Multiple Cylindrical Micromegas

3.1 What is planned for the next funding cycle and beyond?

3.1.1 CEA-Saclay

In the central pseudorapidity region of an EIC detector, the vertexing detector can be complemented by a low material budget MPGD tracker instead of a TPC. The goal is to study the feasibility and the impact of several concentric cylindrical layers of Micromegas tiles for the EIC detector.

The curved Micromegas technology has been successfully deployed for the central tracker of the CLAS12 experiment at JLab. The Micromegas tiles used in CLAS12 have a 1D readout and the material budget per tile is about 0.3% X_0. Starting from this technology, we plan to:

1. Implement several possible detector configurations in the EIC software framework Fun4All and to study the impact on tracking performances. The simulation effort is already started within the context of the EIC Yellow Report. As an example of these studies, Figure 12 shows two possible arrangements of six concentric layers of Micromegas tiles, one with equally spaced and one with three pairs of layers. The preliminary study on the momentum resolution is also shown.
2. Devise a light supporting structure in order to minimize the material budget both in the central in the end-cap regions.
3. Study the impact of different patterns for the 2D readout in terms of spatial resolution, number of readout channels and material budget. CEA-Saclay has studied in collaboration with SBU and BNL zigzag readout patterns within a BNL LDRD program. We plan to assess the impact of this solution for the EIC cylindrical tracker. We also plan to study the large pad readout design proposed by UVa, see Appendix D.1, for Micromegas: a PCB will be bulked at CEA-Saclay with a Micromegas; we will tested its performances with X-rays and the muon telescope and subsequently in beam tests.

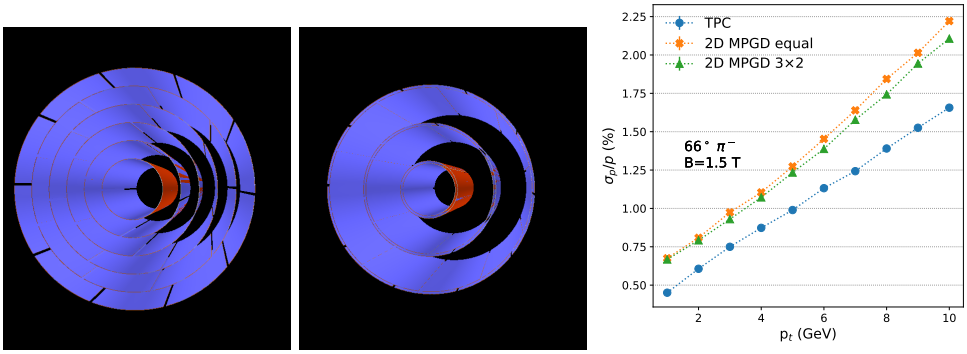

Figure 12: Examples of two possible arrangements of Micromegas layers, i.e. equally spaced (left) and three pairs of layers (center), for a full barrel tracker and the preliminary results on the momentum resolution compared to the TPC solution for the EIC detector (right).

4 Fast Tracking Layer in Barrel Region with Cylindrical μRWELL

4.1 What was planned for this period?

4.1.1 Cylindrical μRWELL studies at Florida Tech

We planned to construct a mechanical mock-up of the smallest cylinder in a tracker barrel. The main motivation is to check if foils can be properly stretched according to our design to produce a stable and uniform cylindrical structure from foils.

4.1.2 Cylindrical μRWELL studies at TU

For this cycle, we planned to:

1. **Build 10 cm $\times$ 10 cm planar μRWELL μTPC prototype:** Build and characterize a 10 cm $\times$ 10 cm planar μRWELL operating in μTPC mode. This detector would be characterization in the TU detector lab using current electronics and DAQ. These results would then serve as input into our ongoing simulation work.
2. **Assess the impact of cylindrical μRWELL trackers on PID detectors:** Study the impact that μRWELL trackers would have on the angular resolution of tracks at a potential DIRC detector. Compare these resolutions to those desired by the PID working groups.
3. **Implement μRWELL support material:** Implement the μRWELL support structure that FIT is building into our current simulation.
4. **Develop slow simulation of μRWELL:** Implement our μRWELL cylindrical trackers into slow simulations where we can more accurately simulate the μTPC operating mode.

4.1.3 Cylindrical μRWELL studies at UVa

For this cycle, we planned to:

1. **Characterisation of μRWELL prototype:** Continue the characterisation of the prototype and the time properties and the non uniformity pattern observed with previous data and look at the JLab Hall

D test data. Moreover, we also planned to test the prototype in Spring 2020 at the Fermilab Test Beam Facility to study the detector performances in high energy hadron beam.

2. **Assembly and preliminary tests of the μRWELL-μTPC prototype:** Complete the procurement of the parts for the μRWELL-μTPC prototype with Field cage from CERN and assemble the detector, instrument the prototype with the new SRS-VMM electronics and study the performances in the mini drift operating mode. Compare performances with the Temple U's field cage free μRWELL-μTPC prototype.

3. **Assembly and preliminary tests of the SRS-VMM readout electronics:** Complete the procurement the minimal SRS-VMM readout electronics, test the new readout electronics on the μRWELL-μTPC prototype in μTPC mode. Start the integration of the new readout electronic system into RCDAQ, the data acquisition software framework supported at BNL by M. Purshke and adopted by the larger EIC tracking detector R&D community.

4.2 What was achieved?

4.2.1 Cylindrical μRWELL studies at Florida Tech

Construction of a Mechanical Mockup for Cylindrical μRWELL Detector: Since the last report, updates have been made to the design of the mechanical mockup for the cylindrical μRWell detector, in particular to the end-ring assemblies (Figs.13,18). The design for the slots which contain the stretching nuts was adjusted to fit nylon nuts. The holes for the closing screws that press the end-ring assembly together were initially designed for 2 mm holes; we instead now go with M3 screws.

Figure 13: Left: Side view of nylon stretching rods inserted into the middle ring of one end-ring assembly. Right: End view of ring assembly with stretching rods (white) and radial closing screws that press the assembly together (black). Screws will be shortened in the next iteration.

The 3D printing of this design was difficult to do locally. Consequently, this printing task was outsourced to the BNL Instrumentation group with help from Bob Azmoun, and the BNL rings are the ones used in this mockup model. The printed rings are generally of high quality, but there is a lack of accuracy with respect to the design parameters, possibly due to shrinkage of the material after printing. It turns out that the design parameters currently also do not have enough tolerances, particularly in accounting for the thicknesses of the foils and o-rings. As received, the frames are sometimes too tight or too loose. The middle rings are machined down at the university machine shop to correct this. These adjustments allow for far better fitting of the components. However, the 1.9 mm diameter o-rings still prove too thick to fit between the rings, so they are removed for the first assembly of this mockup.

For assembly, holes are cut in a 10 mil (250 μm) Cirlex® Kapton foil that correspond to the holes in the rings. The foil is then cut to appropriate size to match the circumference of the inner rings. in our model

this foil represents the μRWELL foil of similar thickness. These same steps are taken for a 2 mil (50 μm) Kapton foil, which represents the drift foil in the model. The Cirlex foil is wrapped around the inner rings, temporarily fixated with screws at the ends and then the two edges are spliced together with adhesive Kapton tape (Fig. 14). This structure proves to be already mechanically quite stable by itself due to the relative thickness of the Cirlex Kapton foil. The middle spacer ring is placed over the Cirlex foil and aligned with the inner holes. Next, the "drift" foil is wrapped around the middle rings and spliced together using adhesive Kapton tape to seal the gap between its edges. The outer rings are then installed around the drift foil and the closing screws are inserted. For this prototype, the holes in the material are tapped to hold the closing screws. Alternatively, they can be secured with nuts. The excess "drift" foil is cut away at both ends to complete the cylinder assembly. Finally, the cylinder is suspended between two plexiglas endplates using thin nylon rods, which are tensioned with nuts against the endplates (Fig. 15). This completes the assembly of the mockup model.

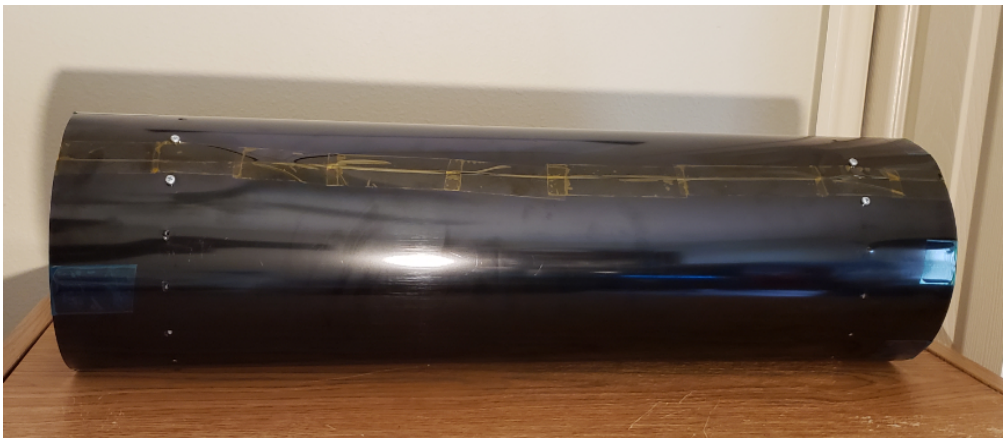

Figure 14: Cirlex Kapton foil wrapped around inner end-rings of μRWELL mechanical mockup. Adhesive Kapton tape splices the two ends of the foil together.

From our first assembly experience, we find that the stretching of the foils poses some challenges. Since the threaded nylon rods are just rods, there is no screw head to easily apply a manual force for stretching. Most of the stretching of the foil must be done by hand before the outer frame is installed as the closing screws are already tightened down. For future designs, we will review if the closing screws should pass through the foils or not. The crimping of the edges as the foil meets the rings is due largely to tightness in installation. The lack of a complete symmetry, as the foil requires adhesive Kapton tape for splicing the edges together, causes an imperfect cylindrical shape that also plays a role in the crimping.

4.2.2 Cylindrical μRWELL studies at TU

1. **Assess the impact of cylindrical μRWELL trackers on PID detectors:** Particle identification at an EIC is going to be critical. In ongoing discussions with the EIC PID groups it has been made clear that good angular tracking resolution will improve the effectiveness of the PID detectors, in particular the DIRC and RICH detectors. We have studied the impact that our fast cylindrical μRWELL trackers would have on the angular tracking resolution in the central region.

   We simulated three detector setups within the EicRoot framework. The first refereed to as "No MPGD", consisted of a silicon vertex tracker, TPC, and the DIRC material volume. In the second setup ("1 MPGD") we inserted two μRWELLs, one just before the TPC inner field cage and the other just outside the outer TPC field cage and before the DIRC. For the third setup ("2 MPGD") we had the μRWELL trackers inserted in front and behind the DIRC. Fig. 16 shows the latter two simulation setups, additional information regarding the simulation details can be found in the appendix C.

   The study was done for π^- particles in a 1.5 T magnetic field for scattering angles of $43^o, 66^o$, and 89^o

Figure 15: Side view of assembled and suspended mechanical mockup for cylindrical μRWELL. Total length (w/o endplates): 60.3 cm; length of the "active area": 44.9 cm; diameter of inner Kapton foil: 16.2 cm; diameter of outer Kapton foil: 19.6 cm.

over a momentum range of 1 to 7 GeV. Figure 17 shows the results of the polar angle resolution ($\Delta\theta$) vs. momentum for pions at $\theta = 43^o$ (similar trends were seen for the other scattering angles). The resolutions of the three detector setups are compared. The left panel shows the θ resolution that would be achieved at the front face of the DIRC, while the right plot shows resolutions that would be measured behind the DIRC. We see a drastic improvement in angular resolution at the front face of the DIRC when there is a μRWELL detector before the DIRC compared to when there is none. As expected, the resolution at the front of the DIRC is insensitive to whether the second tracker is before the TPC ("1 MPGD") or after the DIRC ("2 MPGD"). We find a significant improvement in angular resolution measured behind the DIRC when a μRWELL tracker is inserted after the DIRC. Due to the multiple scattering within the DIRC material, the angular resolution of the track exiting the DIRC is much worst compared to the angular resolution of the track as it enters the DIRC, which suggests having a tracker behind the DIRC could help with the PID performance of the DIRC. From this initial study we found that the DIRC would benefit the most from having 2 cylindrical μRELLs located just before and after it. Of course the absolute value of the angular resolution depends on the detector resolutions, such as the TPC, and should be revisited as detector parameters become finalized.

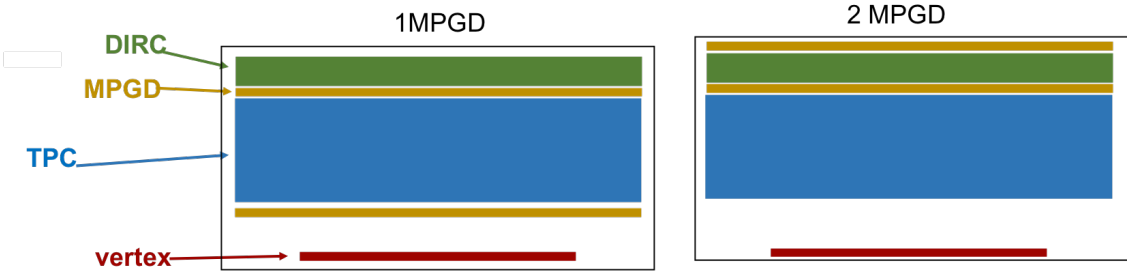

Figure 16: Cartoon showing the various detector setups used in the angular resolution study.

2. **Implement μRWELL support material:** So far our simulation studies have been carried out using cylindrical μRWELLs which have no support materials included. In an effort to move towards a more realistic description of the detectors material budget, we have begun to incorporate the support structure being developed by FIT. Figure 18 shows the FIT support rings and its description within the Fun4All

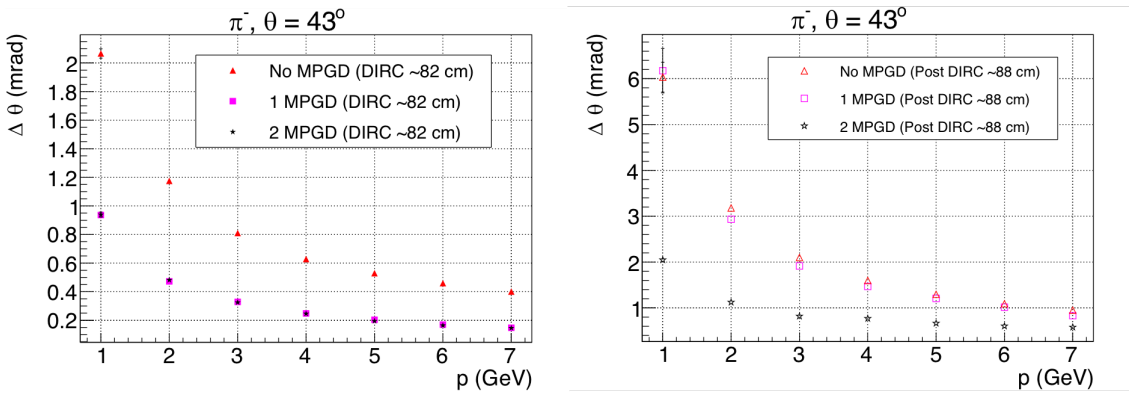

Figure 17: $\Delta\theta$ vs. momentum for π^- at $\theta = 43^o$. Resolutions in the left plot are determined at the front of the DIRC (closer to IP), and the right plot after the DIRC.

simulation/analysis framework. The bottom left image shows 2 cylindrical μRWELLs with the support rings installed. We have completed an initial material budget studies where we assessed the material impact in different η regions with different detector configurations. The plots in the right hand panels in Fig. 18 (a,b) show the radiation length vs. η, where the trackers had radii of 12.5 cm and 80.0 cm. Two μRWELLs similar to this could be used to surround a TPC or silicon barrel. We looked at a couple of things in this study, the first was the impact of the support material. The red lines shows the material budget when the supports are made from a Carbon fiber material, the blue lines when they are made from PEEK, and as a reference point, the black line shows the trackers when there are no support rings included. From this we see that there is not too much difference between PEEK and Carbon fiber, with PEEK being slightly preferred. The second study involved varying the inner (closest to the vertex tracker) tracker length. Panel (a) is the material budget with both trackers having a length of 200 cm, and panel (b) is the resulting budget after reducing the inner tracker length to 120 cm. We can see a clear decrease in the material budget at larger $|\eta|$ when reducing the length of the inner tracker.

3. **Fun4All:** Fun4All and Escalate have been identified as two official EIC simulation frameworks. As a result we have begun working within Fun4All. Our cylindrical μRWELL tracker description, along with the support rings have now been built within Fun4All. We also now are able to project tracks to different locations (i.e. the DIRC).

4.2.3 Cylindrical μRWELL studies at UVa

1. **Characterisation of small planar μRWELL prototype:** The small μRWELL prototype with 2D strip readout was part of the setup in Hall D at JLab during Fall 2019 run for the commission of a DIRC detector for Hall D detector upgrade and later in the standalone GEM-TRD test setup during JLab 2020 Spring run. Unfortunately we had some issues with the readout and DAQ system for these trackers that prevent us to collect good quality data in 2019. The issues were resolved however, the closing of JLab campus as a consequence of COVID-19 lock-down situation has put on hold the testing of this prototype.

2. **μRWELL-μTPC prototype:** As reported in our January 2020 progress report, the design of the μRWELL-μTPC prototype was completed. Procurement of the parts at CERN was expected to happen earlier this year after completion of the UVa portion of the eRD6 FY20 funding. Unfortunately, This was delayed the COVID-19 lock-down situation both at CERN and later at UVa.

3. **Set up of the SRS-VMM readout electronics:** The situation is similar for the SRS-VMM readout system that we acquired at UVa. We had to this day received most of the components of the system purchased from the SRS-Technology company and the CERN store except for SRS power supply crate. The procurement of this item has been delayed because of some production issues from he manufacturer

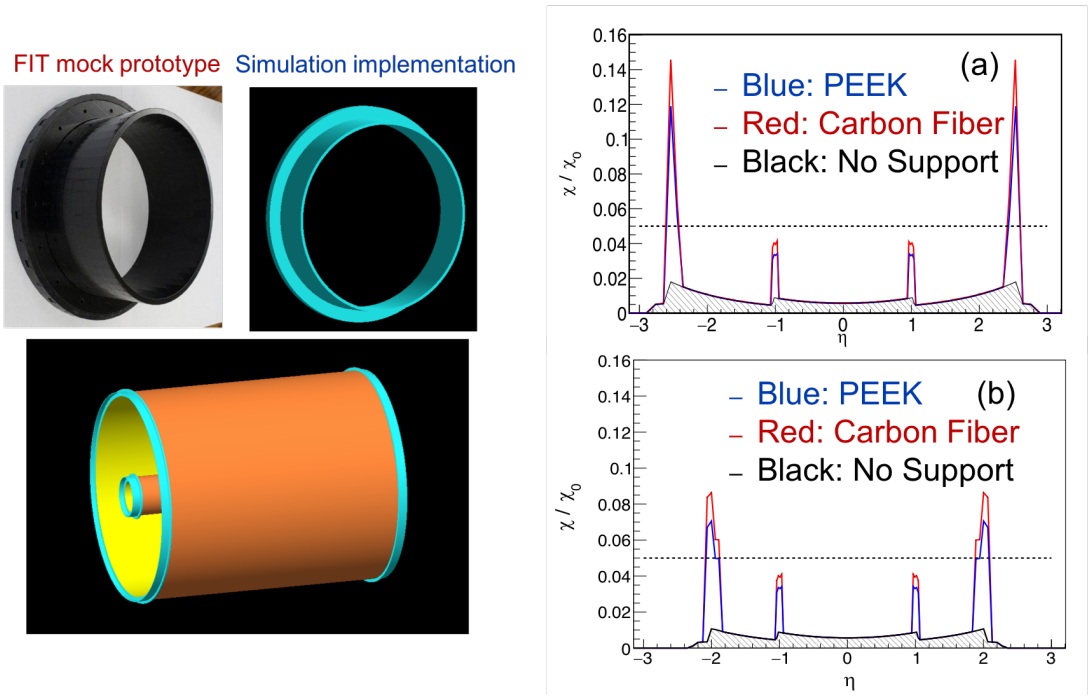

Figure 18: Upper left panel shows Fun4All implementation of cylindrical μRWELL trackers and support rings. Right panel shows material budget for the detectors using different support materials. Panel (a) is for a 200 cm long inner tracker and (b) for a 120 cm long inner tracker.

and later the COVID-19 situation. However, we expect to have the SRS power supply in hand in the next coming weeks and will be able to start the activity.

4. **Small GEM Trackers for cosmic telescope at UVa:** We have assembled two small X-Y strips COMPASS Triple-GEMs detectors that will be used as trackers in the cosmic telescope stand to be set up in our detector lab at UVa. The GEMs are also going to be used as trackers in our scheduled test beam at Fermilab in 2021. Both chambers have been tested and validated with cosmic and in x-ray. We will start putting together the cosmic telescope after we fully resume activity in the lab at UVa.

5. **Development of a novel large-pad & capacitive-sharing readout PCB:** We are exploring a new large-pad & capacitive-sharing anode readout PCB concept to be coupled with Micro Pattern Gaseous Detectors (MPGDs) amplification devices such as GEMs, μRWELLs or Micromegas. This novel readout PCB idea, which is expected to provide excellent spatial resolution with significantly low readout channel count, presents several advantages for various EIC MPGD tracking options. The basic principle of the readout scheme is described in detail in the appendix D.1. We assembled one such 1 cm^2-pad capacitive-sharing readout PCB produced at CERN with a small triple-GEM detector to establish the proof of concept. The specifications of the board are shown on the top Fig. 19 and based on the 5-pad-layers readout design described in appendix D.1. The prototype was tested in x-ray setup at UVa with a 1 mm^2 collimated x-ray source, as shown on bottom left of Fig. 19. The 2D plot of middle left of the figure shows the x-ray beam spot spread over a few readout pads covering an area of 3 cm $\times$ 2 cm. The reconstructed positions of the x-ray hits is shown in the 2D plot of middle right of Fig. 19 and the plot on the right shows a zoomed area of high granularity reconstructed hit positions with 10 μm $\times$ 10 μm histogram bins. We see, as expected a uniformed distribution of the reconstructed positions with no pattern associated to the pad readout geometry which is a strong indication that excellent space point resolution can indeed be expected with this new readout PCB concept. The preliminary results are very encouraging to us to develop further the new idea and test the performances with different MPGD amplification structures (GEMs, μRWELLs or Micromegas).

5-Pad-Layers Large-Pad Readout

- Standard CERN triple-GEM Active area: 90 mm × 90 mm
- Top layer pad pitch: 0.625 mm × 0.625 mm; 0.1 mm inter-pad
- Readout pad pitch: 1 cm × 1 cm; 0.1 mm inter-pad
- DLC: surface resistivity ~20 Mohm

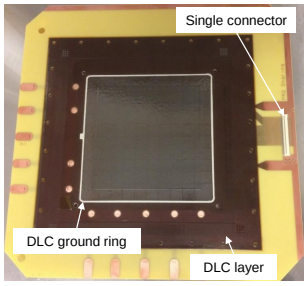

- Average pad hit occupancy: 6 pad (3 × 2) ⇨ average beam size spread on pads over an area of 3 cm × 2 cm
- Size of the reconstructed beam: 3 mm x 3 mm ⇨ strip occupancy / spot size ratio = 67
- Uniform distribution of the reconstructed hits: 2D histogram with 10 µm × 10 µm bin size
  ⇨No pattern correlated to the pad RO geometry
  ⇨Excellent resolution expected with this geometry
- Center of gravity (COG) for position reconstruction

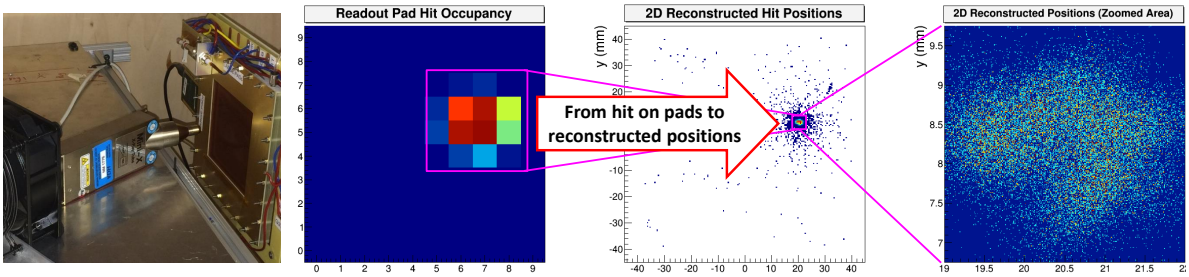

Figure 19: ***(Top):*** Picture of 1 cm^2-pad capacitive-sharing anode readout PCB prototype. ***(Bottom - from left to right):*** Triple-GEM prototype with large-pad anode readout installed in x-ray setup at UVa; Readout pad hit occupancy; Reconstructed hit positions; Zoomed area of the reconstructed positions

4.3 What was not achieved, why not and what will be done to correct?

4.3.1 Cylindrical μRWELL studies at Florida Tech

We are still tracing a leak in our planar 10 cm × 10 cm μRWELL prototype. After fixing a broken glue dispensing machine and gluing the window of this detector, this effort had to be paused due to COVID-19.

4.3.2 Cylindrical μRWELL studies at TU

For this cycle, we were not able to successfully complete these planned activities:

1. **Build 10 cm × 10 cm planar μRWELL μTPC prototype:** This activity experienced an initial set back due to delays in transferring the awarded money to TU, which was needed to procure the CERN μRWELL kit. This activity was then further delayed to to the COVID-19 outbreak which left TU's detector lab inaccessible. We do know have the requested money and should be able to access our detector lab by July. We are also now placing our purchase order with CERN.
2. **Simulate μTPC mode:** In the advent of the EIC Yellow Report meetings, we have adopted the Fun4All simulation and analysis framework, which is currently used by sPHENIX, to migrate our simulation work to. We have now setup our μRWELL cylindrical trackers and their initial support material within Fun4All. We will now begin to implement parameterizations needed to simulate a μTPC mode.

4.3.3 Cylindrical μRWELL studies at UVa

For this cycle, we were not able to successfully complete these planned activities:

1. **Characterisation of μRWELL prototype:** We have been unable to collect good quality data with the μRWELL prototype during the Fall 2019 and Spring 2020 JLab Hall D run due to some issues with the readout system and to the lock-down imposed by the COVID-19 respectively. We will resume characterization of the prototype at JLab and in test beam at FNAL during the course of 2020 and 2021 to complete the study of the 2D strips μRWELL prototype.

2. **Assembly and preliminary tests of the μRWELL-μTPC prototype:** The procurement of the parts of μRWELL-μTPC prototype was delayed because of the slow process of getting UVa FY20 awarded funding money from BNL to UVa. Later the COVID-19 lock-down at CERN and at UVa further delayed the activity. We plan to resume the R&D project when the lock-down restrictions are lifted. Moreover we anticipate some changes in the initial plan to include the integration of the novel large-pad readout board into the μRWELL-μTPC prototype design.

3. **Assembly and preliminary tests of the SRS-VMM readout electronics:** The delivery of this SRS-VMM power supply crate has been delayed for almost a year, initially due to production issues with the manufacturer and later by the COVID-19 situation. We were just notified this week by CERN that the item is now available and will be shipped to UVa in the coming weeks. We plan to quickly set up the SRS-VMM system and test it with our small GEM and μRWELL prototypes.

The overall impact of the COVID-19 situation on the R&D activities at UVa is decribed in more detail in the Critical Issues section 7.6.

4.4 What is planned for the next funding cycle and beyond?

The ultimate goal of this joint effort between Florida Tech, Temple U. and UVa is to design and build a fully operational small cylindrical μRWELL prototype and test it in a beam at Fermilab by July 2022. In this development, Florida Tech will take on the mechanics, Temple will be responsible for electronics and DAQ, and UVA will design the μRWELL/readout and drift foils. We anticipate that design and construction of this prototype will occupy at least the entire FY21 funding period. The R&D plans and milestone to reach that goal are described in more details in Sec. 10.2 below.

4.4.1 Cylindrical μRWELL studies at Florida Tech

See Sec. 10.2.3.

4.4.2 Cylindrical μRWELL studies at TU

Regarding our projects that have already been funded, we plan to:

1. **10 cm $\times$ 10 cm μRWELL operating in μTPC prototype:** Complete the assembly of our 10 cm $\times$ 10 cm planar μRWELL prototype operating in μTPC mode.

2. **Simulate μRWELL operating in μTPC mode:** Continue to develop our μRWELL cylindrical tracker simulation within the Fun4All framework. This includes implementing a parameterization for μTPC operating mode and continuing to iterate on the μRWELL support material.

3. **Validate EicRoot studies:** Many of our simulations have been done within EicRoot, we would like to validate these studies within Fun4All and under various magnetic fields. One particular study we would like to verify is the impact on the tracking resolution at PID detectors.

4.4.3 Cylindrical μRWELL studies at UVa

For the coming cycle of FY2021 and beyond, we plan to:

1. **SRS-VMM readout electronics:** Set up the SRS-VMM readout electronics and associated DAQ and decoding software. We plan to test this new electronics with GEM and μRWELL prototypes. With this study to plan to demonstrate that VMM3 will be a viable candidate for EIC MPGD trackers at the July 2021 EIC Detector R&D Committee Meeting.
2. **Characterization of μRWELL prototype with X-Y strip readout:** Resume the characterisation of the prototype, in the x-ray setup at UVa as well as in test beam at JLab and Fermilab to finalize the studies of the spatial resolutions, timing performances and response uniformity of the prototype. We plan to complete the study and present the final results at the July 2021 EIC Detector R&D Committee Meeting.
3. **Development of High-Resolution Capacitive-Sharing Anode Readout for MPGD detectors:**

   We plan to assemble a second μRWELL, equipped with the novel large-pad anode readout PCB described in **appendix D.1**. This novel readout technology has several advantages over the traditional X-Y strips readout for large area MPGD detectors i.e. excellent spatial resolution with significantly less channel counts, the low fabrication cost and low risk fabrication. We have identified two areas where further R&D are required to fully validate the concept.

   - **Proof of concept of large-pad & capacitive-sharing readout with μRWELLs:** We have demonstrated that the large-pad readout concept works well with Triple-GEM detector. However, the amplification structure of GEM are being quite different from a μRWELL therefore, a dedicated R&D is required to demonstrate that this large-pad readout concept will equally work with μRWELL technology. We plan to equip the μRWELL-μTPC prototype with a dedicated large-pad readout and study the performances with cosmic and x-ray source at UVa as well as in test beam at Fermilab.
   - **Minimisation of the capacitance noise and cross-talks:** The second area we would like to investigate is new ideas that we have to minimize the capacitance induced noise and cross talk effect inherent of the large pads. The first study that we plan to carry out is to investigate the impact of the inter-pad capacitance noise and cross talk is described on the sketch of Fig. 36 in the appendix section. D.3. where we plan to study different pad geometry but with the same pad size, on a single readout board. This initial study will quickly educate us on the best approach to minimize the capacitance noise and cross talk effect for larger pad size. In addition, moving from a plain pad to the concentric squared could be the solution to reduce the material budget.

   We plan to conclude the initial aspect of the studies of large-pad, capacitive-sharing readout and present the conclusions at the July 2021 EIC Detector R&D Committee Meeting.
4. **Design and construction of a small size cylindrical μRWELL prototype:**
   See Sec. 10.2.1.

5 End Cap Trackers with GEMs

5.1 What was planned for this period?

5.1.1 Florida Tech Large Carbon Fiber GEM Prototype with zigzag readout

We wanted to check if the detector can hold HV after inserting Kapton rings as spacers into the induction gap and perform quality control tests on the refurbished low-mass prototype. If not, we planned to investigate additional stabilization measures.

5.1.2 UVa Large GEM Prototype with 2D U-V readout

We planned to acquire different types of zebra strips to be tested with the large EIC GEM prototype as we suspected the type of zebra strips that we used for the current prototype, to be one of the reasons of poor performance in a spatial resolution that we observed from 2018 FNAL test beam data.

5.2 What was achieved?

5.2.1 Florida Tech Large Carbon Fiber GEM Prototype with zigzag readout

Refurbishment of low-mass EIC Forward Tracker GEM detector prototype: Even after inserting Kapton rings to partially fill the induction gap, the gap remained shorted. Various measures were then applied to stretch the foils better, but did not succeed. In particular, we observed that a stretched foil would lose tension after several days. This prompted us to reopen the detector to investigate. We found that some of the hex nuts used for stretching had apparently rotated during tensioning and abraded the inner frames (Fig. 20 left). In the detector corners, the frames were also bent at the ends which compromised foil stretching (Fig. 20 right). This is mainly due to the fairly thin arch in the frame cutout for the stretching nut and screw.

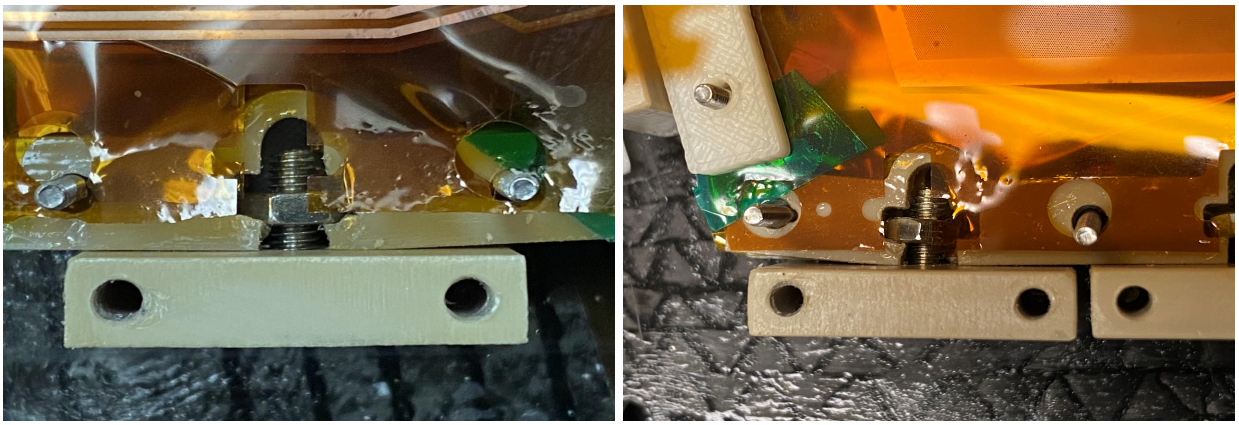

Figure 20: Damages observed on inner frames of large carbon fiber GEM prototype from foil stretching. Left: Inner frame cutout abraded by stretching nut. Right: Bent inner frame with arch in detector corner.

Fig. 20 shows also that maximum possible stretching was applied in the current detector with the inner frames pulled all the way flush against the pull-out posts. To increase the available margin for stretching, the inner faces of the posts were manually thinned to increase the gap between frames and post (Fig. 21).

5.2.2 UVa Large GEM Prototype with 2D U-V readout

We have made very little progress with the large EIC GEM prototype.

5.3 What was not achieved, why not and what will be done to correct?

5.3.1 Florida Tech Large Carbon Fiber GEM Prototype with zigzag readout

Due to the ongoing detector refurbishment, we have not yet been able to commission the detector. On the simulation side, we are still struggling with extracting information on track positions from EICroot to

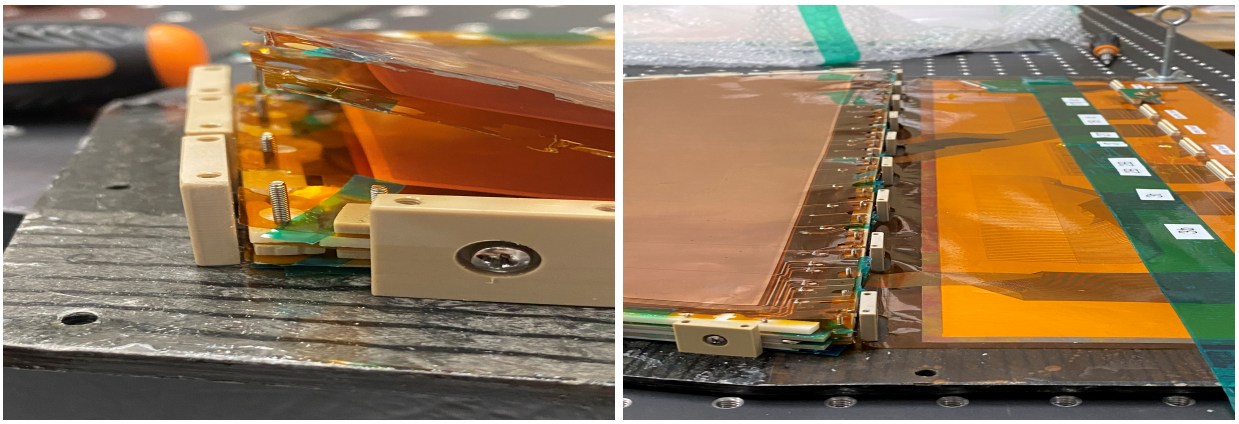

Figure 21: Thinned pull-out posts for stretching GEM foils. Left: Comparison of thinned pull-out in front with two original pull-outs behind it. Right: Row of thinned pull-outs at wide end.

calculate residuals as function of detector material. This is due to the complexity of the EICroot track fitting code, loss of our graduate student Matt Bomberger, who decided to leave graduate school for medical reasons, lack of in-house post-doctoral support from the project, and limited availability of EICroot experts.

5.3.2 UVa Large GEM Prototype with 2D U-V readout

The procurement of different type of zebra strips to test on the large GEM with U-V strip readout has been affected by the delay caused by the long process of getting UVa FY20 awarded funding money from BNL to UVa and later the COVID-19 lock-down at

5.4 What is planned for the next funding cycle and beyond?

5.4.1 Florida Tech Large Carbon Fiber GEM Prototype with zigzag readout

See Sec. 10.3.2.

5.4.2 UVa Large GEM Prototype with 2D U-V readout

We plan to resume and complete the study of the prototype signal response. We will procure different types of zebra strips to test with the prototype in x-ray. If this preliminary test is conclusive, we plan to bring the to FNAL a beam test in 2021 and study the spatial resolution performances with 120 GeV proton beam.

6 Developments for high momentum hadron identification at EIC

6.1 What was planned for this period?

6.1.1 MPGD sensors of single photons at INFN Trieste

The construction and characterization of the second version of the prototype is foreseen for the year 2020.

6.1.2 New Photocathode Materials development at INFN Trieste

The original activity planning for 2020 was including:

- The construction of THGEMs formed with two layers, where only the upper layer is exposed to hydrogenated ND coating process and its full characterization.
- Further studies dedicating to define the properties of ND powders with different characteristics are planned.

Both items have been matched during the first month of the current year and reported about in the January 2020 report.

The successful activity recalled above, has suggested further steps for the second part of the current year, as anticipated in the January 2020 report. This includes:

- The heat treatment, that allows recovering the required electrical rigidity of HND coated THGEMs, has been applied in air atmosphere. Some reduction of the QE is observed, most likely related to oxidation in air. The heat treatment protocol needs to be modified heating in inert atmosphere. Then, it will be verified if the effective QE is preserved.
- The measurements to establish the effective QE of HND photocathodes will be completed.
- The investigation of ND powder parameters infuencing the QE performance will be continued.
- First measurements of HND radiation hardness will be performed in the ASSET setup at CERN.

6.1.3 Large mirrors development at Stony Brook

The installation and commissioning of mirror coating equipment was planned in the present funding cycle.

6.1.4 New Radiator Studies at Stony Brook

Studies of meta-materials suited for the application of Cherenkov photon detection was planned. Students working on the project were to model appropriate materials.

6.2 What was achieved?

6.2.1 MPGD sensors of single photons at INFN Trieste

This development is fully based on laboratory activities, seriously affected by the restrictions imposed by the pandemic emergency (Sec. 6.3.1). Only the activity of the period January-February 2020 can be reported.

In Janury 2020, we reported that the activity has partially deviated from the planning. This deviation has been suggested by the analysis of the test beam data and the further laboratory studies of the prototype. The only serious limitation observed in studying the first prototype is related to the noise level and we have indicated the two action lines started to overcome this limit. They are recalled in the following updated to the status at the end of February, the last working month.

- The detailed analysis of the potential noise sources in the first prototype version and the design of the second version of the prototype modified with the goal of minimizing the noise. The design, mainly related to the anode PCB, which is also the support of the micromesh of the MICROMEGAS stage of the hybrid MPGD, has been completed and it is now ready for submission (Fig. 22).

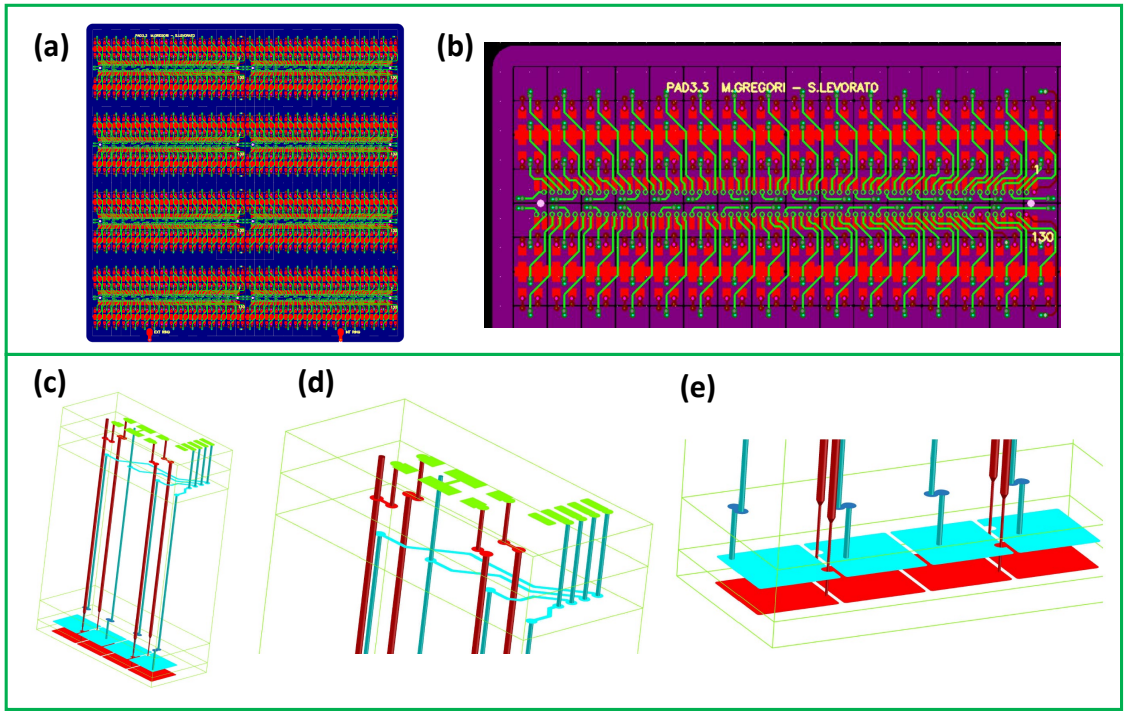

Figure 22: Design of the PCB for the resistive micromegas, improved version. (a) Connector face. (b) Zoomed view of a portion of the connector face; the pads for the SMD resistors are visible. (c) The vertical vias. (d) Zoomed view of a portion of the vertical vias at the connector face. (e) Zoomed view of a portion of the vertical vias at the pad face, facing the micromegas micro mesh.

- The VMM3 ASIC is a novel chip designed for MPGDs with features promising for our application. In fact, the low noise figure and the capability of effective coupling with detectors in a wide capacity range are specifically beneficial to our single photon detection application, namely an application requiring single photoelectron detection, performed by a hybrid MPGD where the last multiplication stage is by a MICROMEGAS, namely a relatively high capacitance detector. Moreover, the chip architecture is designed for trigger-less operation, namely adequate for usage in upo-to-date DAQ systems. We have acquired two pieces of the MMFE1 board, a VMM read-out board developed in the context of the ATLAS NSW project, design to exploit all the most relevant VMM3 features, including the good noise figures. In parallel, we have designed a dedicated MICROMEGAS prototype, designed according to our architecture of resistive micromegas changing the connectors so that part of the detector can be read with the MMFE1 board and part using an SRS-APV25 card in comparative exercises (Fig. 23). The PCB design is now ready for submission.

6.2.2 New Photocathode Materials development at INFN Trieste

This development is fully based on laboratory activities, seriously affected by the restrictions imposed by the pandemic emergency. Only the activity of the period January-February 2020 can be reported.

Nevertheless, during the first months of year 2020, all the activities planned for FY2020 have been completed and reported about in the January 2020 report and, therefore, the related milestone had been matched.

The successful activity recalled above, has suggested further steps for the second part of the current year, listed in Sec. 6.1.2. Their preparation started in January and February and unfortunately suspended due to the laboratory shutdown.

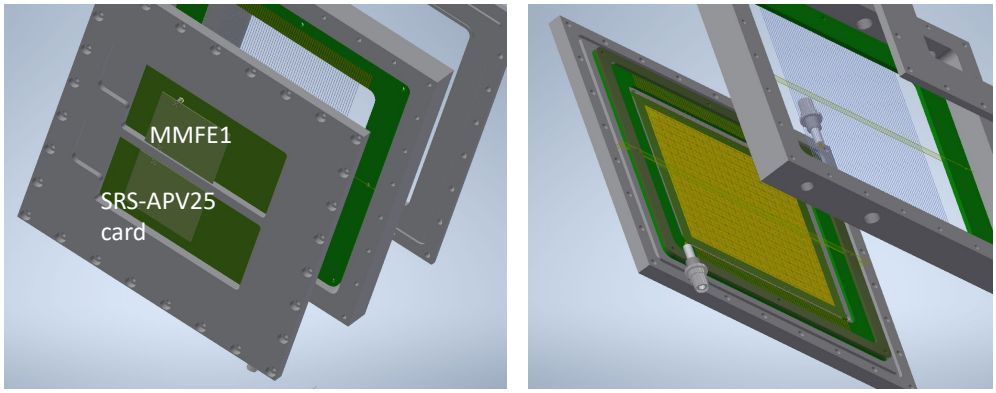

Figure 23: Principle design of the dedicated prototype micromegas for comparative studies of detector readout via VMM3 implemented in the MMFE1 board and via APV25 implemented in the SRS-APV25 board.

6.2.3 Large mirrors development at Stony Brook

The electron-/ion-beam equipment has been installed.

6.2.4 New Radiator Studies at Stony Brook

The development of models and its application in the FEM software COMSOL has continued. We are focusing on calculating the propagation of electromagnetic waves (`emw`) through embedded objects. The `emw` correspond to light waves at various wavelengths. The objects under consideration are spheres of a certain material surrounded by spherical layers of equal or different material. The size of the spheres makes them to be called nano-spheres.
The spheres were varied in their radius with the largest radius of $r_f = 240$ nm and successively subdivided into 8 sections (1 core and 7 shells) with radius and thickness 30 nm. The materials of each layer alternate, between "lossless" silica with $\epsilon_{\text{silica}} = 2.04$ and TiO_2 with $\epsilon_{TiO_2}(\lambda) = 5.913 + \frac{0.2441}{(\lambda^2 - 0.0803)}$. The innermost layer is made of Si.
Example results of the FEM calculations can be seen in Figs. 24. We furthermore modeled an array of 2×2 of above described many-layered spheres and the repeated propagation of `emw` was calculated. An example of the calculations can be seen in Fig. 25.
A neural network for the massive calculation within the large parameter space is being developed. In addition, the so-called T-matrix formalism is developed for analytically calculating the scattering of `emw` off of an arrangement of nano-spheres. This will allow us to generate a large training and verification sample to be used in the neural network. In parallel, the FEM will be used to verify the correct application of the T-matrix formalism.
We obtained a license agreement with Sandia Lab which allows us to make use of the MIRaGE software. As a reminder, MIRaGE lets users start by telling it the optical property they want - how their metamaterial needs to interact with light - and their starting materials. MIRaGE generates designs that match those criteria from a library of more than 100 templates. Or, users can draw their own designs, and the program will check them for errors. At the time of this write-up the license agreement has been signed between SBU and Sandia labs and we are awaiting the release of the software via the distribution to authorized users.

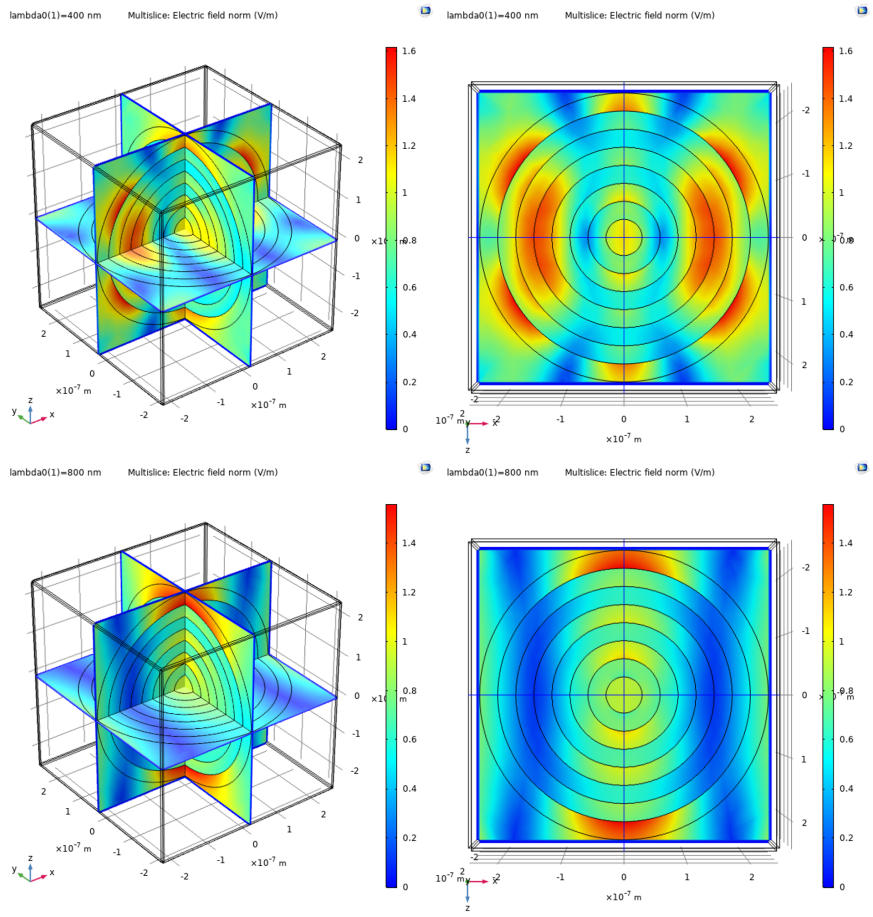

Figure 24: Upper and lower panel are for wavelengths of 400 nm and 800 nm, respectively.
Left: 3-d sliced view of a planar wave propagating along the positive z-axis. Right: same object but viewed from top showing the x-z-plane.

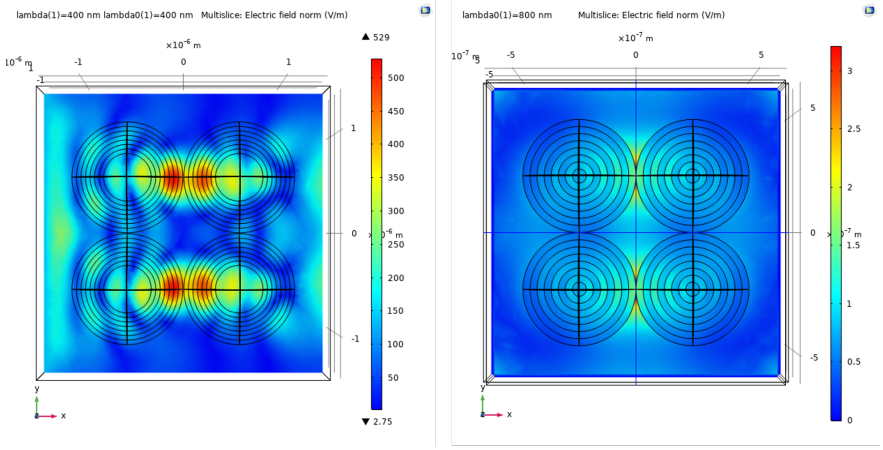

Figure 25: Top down view of a plane wave propagating from the left along the x axis through an arrangement of nano-spheres. Left and right are for wavelengths of 400 nm and 800 nm, respectively.

6.3 What was not achieved, why not and what will be done to correct?

6.3.1 MPGD sensors of single photons at INFN Trieste

This development is fully based on laboratory activities, seriously affected by the restrictions imposed by the pandemic emergency. Laboratory activities have been stopped at INFN Trieste and at INFN Bari at the beginning of March and restarting is expected in September. Therefore, more than 50% of the current year is of forced inactivity and the planned work has to be reported to the following year.

In particular: The construction of the second version of the prototype has been started but not completed and, as a consequence, the prototype will not be characterized in the current year. The related milestone will not be matched.

6.3.2 New Photocathode Materials development at INFN Trieste

This development is fully based on laboratory activities, seriously affected by the restrictions imposed by the pandemic emergency. Only the activity of the period January-February 2020 can be reported. The activities of period October 2019- February 2020 include all what has been originally planned for the FY2020.

The preparation for the extra activities, proposed in January 2020 on top of the ones originally foreseen and already completed by the time of the previous report, has started and unfortunately suspended due to the laboratory shutdown. This activity is moved to year 2021.

6.3.3 Large mirrors development at Stony Brook

The startup of the evaporator unit was planned for the first quarter of this year, however, due to the COVID-19 related shutdown of lab activities no work could be performed. At the time of this write-up we have entered phase-2 return allowance from SBU. This gave us the chance to enter the lab for the first time in mid-June and we are resuming our activities.

6.3.4 New Radiator Studies at Stony Brook

None.

6.4 What is planned for the next funding cycle and beyond?

6.4.1 MPGD sensors of single photons at INFN Trieste

The activity planned for year 2021 has to include a large fraction of the 2020 planning, that cannot be performed due to the current emergency shutdown. The completion of the construction and characterization of the second version of the prototype is now foreseen for the year 2021.
Related milestone
September 2021: The completion of the laboratory characterization of the second version of the photon detector with miniaturized pad-size.

Novel item: An exploratory study about the configuration of the MPGD pads will be attempted aiming at reducing the discharge rate. Electrostatic calculation will be performed. If they provide promising indications, laboratory tests will be scheduled.

6.4.2 New Photocathode Materials development at INFN Trieste

The activity planning includes the items proposed for the second half of 2020, that cannot be performed due to the emergency shutdown, namely:

- The heat treatment, that allows recovering the required electrical rigidity of HND coated THGEMs, has been applied in air atmosphere. Some reduction of the QE is observed, most likely related to oxidation in air. The heat treatment protocol needs to be modified heating in inert atmosphere. Then, it will be verified if the effective QE is preserved.
- The measurements to establish the effective QE of HND photocathodes will be completed.
- The investigation of ND powder parameters influencing the QE performance will be continued.
- First measurements of HND radiation hardness will be performed in the ASSET setup at CERN.

. Moreover, a novel item is added: the realization of a complete small size prototype of a MPGD-based photon detector with hydrogenated nanodiamond power photocathode.

Related milestone
September 2021: Complete small size prototype of a MPGD-based photon detector with hydrogenated nanodiamond power photocathode.

6.4.3 Large mirrors development at SBU

The installation has been finalized pending some modifications and the graduate student working on the project for his master thesis will perform the commissioning of the device in the remaining funding cycle.

6.4.4 New Radiator Studies at Stony Brook

We are awaiting the release of the Mirage software so that the students assigned to this project might be able to find a solution to the meta-material problem. In parallel we are continuing to develop our own neural network framework.

7 Critical Issues: Impact of COVID-19 pandemic

7.1 Brookhaven National Lab

7.1.1 How did the COVID-19 pandemic affect progress of your project?

BNL halted normal operations around March 20th and went into "min-safe" mode, effectively barring any scientific staff from entering the site. As a result, our group has since only been able to conduct work from home and by teleconferencing. The lab has starting a gradual/phased reopening in mid-June, but members of our group will not be permitted to return to work until mid-July. Even then, the amount of time allowable on site will be limited and telecommuting will be encouraged. At this point the impact on future work is not clear.

7.1.2 How much of your FY20 funding could not be spent due to the closing of facilities?

We received $37,500 in new funding in FY20 compared to our funding request of $75,000 (i.e., 50%). As of early June we have spent $15,777 of these funds on materials, PCB fabrication and technical support.

We had intended to use the remaining $21,723 (which includes overhead, resulting in $14,500 in spendable funds) to partially support our test beam effort that was mostly covered by our MPGD LDRD in order to test some preliminary designs of readout boards for our TPC prototype. Hopefully these funds can now be carried over into FY21 to do these tests next year.

7.1.3 Do you have running costs that are needed even if R&D efforts have paused?

No. Other than pre-existing or newly placed orders we do not have any ongoing costs during the shutdown.

7.2 Florida Tech

7.2.1 How did the COVID-19 pandemic affect progress of your project?

As the occupancy of our high-bay laboratory is low, some hardware activity could continue after the statewide stay-at-home order was lifted in Florida in early May. As of June 15, the university has resumed regular operation as long as social distancing measures and CDC guidelines are observed.

7.2.2 How much of your FY20 funding could not be spent due to the closing of facilities?

Most of the funding is for students and stipend payments were continued. Also procurement for the mechanical mock-up continued.

7.2.3 Do you have running costs that are needed even if R&D efforts have paused?

Student stipends.

7.3 INFN Trieste

The critical issues concerning the 2021 activities are related to the level of recovery of the standard working conditions at INFN by September 2020. Any incompleteness in the restoration of standard working conditions can result in further delays.

The request support for year 2021 has been kept at the minimum needed to perform the planed activities. It is centered on the needed manpower. Therefore, a reduction of the resources requested would result in an activity delay or cancellation (according to the level of the cut).

7.3.1 How did the COVID-19 pandemic affect progress of your project?

The INFN-Trieste tasks are fully based on laboratory activity seriously affected by the restrictions imposed by the pandemic emergency. Laboratory activities have been stopped at INFN Trieste and at INFN Bari at the beginning of March and restarting is expected in September. Therefore, at least 50% of the current year is characterized by forced inactivity and a large fraction of the planned work has to be moved to 2021.

7.3.2 How much of your FY20 funding could not be spent due to the closing of facilities?

A relevant fraction of the funding for consumable and travelling has not / will not be spent. In particular: consumable - 4000$ (over 8000$ assigned) not spent travelling - 5000$ (over 10000$ assigned) not spent.

7.3.3 Do you have running costs that are needed even if R&D efforts have paused?

The manpower funding of 20,000 $ has been used because the postdoc support has to be continued also in the emergency shutdown period.

7.4 Stony Brook University

7.4.1 How did the COVID-19 pandemic affect progress of your project?

The COVID-19 situation created the shutdown of all lab activities starting from mid-March in 2020. The consequence was the stop of the start-up process for the evaporator as well as the planned commissioning activities.
The planning process for testing the gating grid structure was impacted, too.

7.4.2 How much of your FY20 funding could not be spent due to the closing of facilities?

None of the spending of FY20 funding was paused. We were continuing the design of the gating grid and "only" the planning stage for the test at ANL is on hold.

7.4.3 Do you have running costs that are needed even if R&D efforts have paused?

None.

7.5 Temple University

7.5.1 How did the COVID-19 pandemic affect progress of your project?

We could not begin or complete our μRWELL μTPC prototype work. We had an initial delay due to receiving the awarded money. Once we did receive the money, The COVID-19 pandemic forced Temple U. to close their labs. Labs are expected to reopen by July and this activity can then resume.

7.5.2 How much of your FY20 funding could not be spent due to the closing of facilities?

Come July, we will have spent the money awarded to for the planar 10 cm $\times$ 10 cm μRWELL detector operating in μTPC mode.

7.5.3 Do you have running costs that are needed even if R&D efforts have paused?

Yes, the 10% partial postdoc salary.

7.6 University of Virginia

7.6.1 How did the COVID-19 pandemic affect progress of your project?

The overall impact of he COVID-19 so far was a delay by a couple of months of the planned eRD6 activities at UVa. The acquisition of μRWELL operating in μTPC mode was significantly delayed as well as the

procurement of SRS-VMM electronics power supply and the zebra strips that we planned to test with the large U-V GEM prototype. The test beam plans at JLab and FNAL to complete the studies of the μRWELL prototype with X-Y strips readout has also been postponed as well. These activities are now slowly resuming and we have started to place the order for some of the items that needs to be procured.

7.6.2 How much of your FY20 funding could not be spent due to the closing of facilities?

The bulk of the eRD6 money awarded to UVa for the current FY20 was for procurement of μRWELL, small GEM trackers, zebra strips and SRS-VMM electronics. As of today the order has been placed for most of these items and some of them such as the small GEM trackers have been delivered and GEMs have been assembled and tested. We used a portion of the travel money for travel to JLab during the Fall 2019 and Spring 2020 test beam in Hall D at JLab.

7.6.3 Do you have running costs that are needed even if R&D efforts have paused?

We don't have running cost that are needed while these efforts are paused.

8 Manpower

8.1 Brookhaven National Lab

Our total manpower effort on MPGDs for EIC, which includes eRD6 as well as other activities, is listed below. All scientific and engineering manpower is being supported by internal BNL funds. Funds are requested from eRD6 for technical support.

8.1.1 Total manpower effort for MPGD R&D

- 2 Senior Scientists: Martin Purschke (0.2 FTE), Craig Woody (0.2 FTE)
- 1 Scientist: Alexander Kiselev (0.4 FTE)
- 1 Physics Associate: Bob Azmoun (0.6 FTE)
- 1 Electronics Engineer: John Kuczewski (0.1 FTE)
- 1 Technician: Bill Lenz (0.5 FTE).

8.1.2 Manpower effort for eRD6 R&D

- 2 Senior Scientists: Martin Purschke (0.1 FTE), Craig Woody (0.1 FTE)
- 1 Scientist: Alexander Kiselev (0.2 FTE)
- 1 Physics Associate: Bob Azmoun (0.2 FTE)
- 1 Electronics Engineer: John Kuczewski (0.1 FTE)
- 1 Technician: Bill Lenz (0.3 FTE).

8.2 Florida Tech

- Marcus Hohlmann, Professor, 0.25 FTE, not funded under this R&D program.
- Brendan Steffens, physics graduate student (Ph.D.), funded Jan-May 2020 by this R&D program. Brendan substituted on short notice for Matt Bomberger, who had to leave the program.
- Jerry Collins, physics graduate student (M.S.), funded from spring 2019 through summer 2020 (partially) by this R&D program.
- Merrick Lavinsky, new physics graduate student (Ph.D.), funded in summer 2020 by this R&D program.

8.3 INFN Trieste

From INFN Trieste:

- C. Chatterjee (Trieste University and INFN, PhD student), 0.2 FTE
- S. Dalla Torre (INFN, Staff) 0.2 FTE
- S. Dasgupta (INFN, postdoc) 0.4 FTE
- S. Levorato (INFN, Staff) 0.2 FTE
- F. Tessarotto (INFN, Staff) 0.2 FTE
- Triloki (ICTP and INFN, fellowship) 0.5 FTE

The contribution of technical personnel from INFN-Trieste is also foreseen according to needs.

From INFN BARI:

- Grazia Cicala (NCR staff and INFN) 0.3 FTE
- Giuseppe Casamassima (INFN, Staff) 0.3 FTE
- Teresa Ligonzo Teresa (Bari University and INFN, senior scientist) 0.4 FTE
- Antonio Valentini (Bari University and INFN, professor) 0.3 FTE

Globally, the dedicated manpower is equivalent to 3 FTE.
The effective FTE during the present reporting period is reduced to approximately one third due to the restrictions related to the pandemic emergency.

8.4 CEA-Saclay

All senior scientific and engineering manpower is being supported by internal CEA fund. Funds are requested from eRD6 for technical support. Post-docs and PhD students are not funded under the eRD6 program.

- Physicists: Francesco Bossù (0.2 FTE), Maxime Defurne (0.1 FTE), Franck Sabatié (0.05 FTE)
- Engineer: Stephan Aune (0.1 FTE), Maxence Vandenbroucke (0.1 FTE)
- Post-doc: Qinhua Huang (0.7 FTE)
- PhD students: Aude Glaenzer (0.3 FTE), Maxence Revolle (0.5 FTE)

8.5 Stony Brook University

- K. Dehmelt, Research Associate Professor, 0.3 FTE
- T. K. Hemmick, Professor, 0.1 FTE
- P. Garg, Research Assistant Professor, 0.1 FTE
- A. Kulkarni, Grad student, 0.75 FTE
- S. Park, Postdoc, 0.1 FTE
- V. Zakharov, Grad student, 0.5 FTE
- A. Zhang, Research Assistant Professor, 0.1 FTE

None of the personnel is funded under this R&D program.

8.6 Temple University

- B. Surrow, Professor, 0.1 FTE
- M. Posik, Assistant Research Professor, 0.1 FTE
- A. Quintero, Post-doc, 0.1 FTE
- J. Nam and N. Lukow, graduate student, 0.1 FTE

8.7 University of Virginia

None of the labor at UVa is funded by EIC R&D. The workforce is listed below:

- N. Liyanage; Professor; 0.1 FTE
- K. Gnanvo; Senior Research Scientist; 0.3 FTE

9 External Funding

9.1 Brookhaven National Lab

All scientific and engineering manpower is being supported by internal BNL funds. However, technical support for our eRD6 activities requires support from eRD6 funds.

Additional work on R&D on Micropattern Detectors for EIC is also being provided by a BNL LDRD in collaboration with Saclay and Stony Brook. This is supporting our continued work on zig-zag readouts with GEMs and Micromegas and we do not request any funding for this effort from EIC R&D funds. However, our proposed work on TPC R&D for EIC would not be covered under LDRD funds. It must be noted that our LDRD project will end in Feb. 2021 and we will no longer have any funding for the development of interleaved anode patterns specialized for a TPC.

9.2 Florida Tech

None.

9.3 INFN Trieste

A support of 20 keuro for the year 2020 has been granted by INFN. INFN has also provided the matching resources to extend the postdoc position to one full year.

A support of 25 keuro will be requested for the year 2021, as well as matching resources to extend the postdoc position to one full year.

9.4 Stony Brook University

There is no external funding for this R&D effort.

9.5 Temple University

As of this writing no external funding has been used for eRD6 related projects.

9.6 University of Virginia

None

10 eRD6 R&D Proposals for FY21

10.1 R&D on EIC TPC

TPC Readout Studies at BNL and Yale: The goal of our R&D program is to investigate various high performance options for a TPC endcap readout. This includes the choice of a particular avalanche technology, the geometry of the charge collection anodes, and an appropriately chosen gas mixture. The selection of MPGDs as the gain element has many appealing features, including low mass, low profile, low cost, and many configuration possibilities. Additionally, each type of MPGD provides its own unique benefits. The structure of the charge collection anode (specifically the pitch) carries with it particular importance since this will directly influence the number of required electronics channels, which is the costliest part of the detector by far. The motivation to reduce channel count may also be driven by the need to minimize the material budget of the TPC. Finally, the choice for a given working gas has many implications on various aspects of the detector performance, including dE/dx, attachment, diffusion, IBF, etc. The gas mixture must also be suitably paired with the avalanche and readout elements.

We propose to examine optimal combinations of these three components to address the needs of a TPC readout at the EIC. In particular, we have investigated interleaved (i.e., zigzag shaped) anode geometries, which have relatively large pitch (2-3mm), but maintain excellent position resolution approaching 50μm. In the past, this work was mostly applied to 1D readouts for planar detectors, where a simple focus on optimizing the resolution was employed. However, to develop this concept for TPC's the channel occupancy, as well as the directionality of the sensitive coordinate must be taken into account. At the inner radial region of the endcap, for instance, one may want to reduce the occupancy by increasing the channel count, which will compromise the resolution to some extent. In addition, though the most sensitive coordinate is along phi, some level 2D high resolution space points would also be desirable for improved track reconstruction. Finally, the linearity of response of a readout plane that must satisfy all of the prior concerns must also be addressed. In principle, so-called pad response functions may be determined for a given readout, but we have determined that they may be avoided altogether with an appropriately designed anode.

To determine the best combination of avalanche scheme, anode design, and gas mixture, we propose to conduct this R&D in the following steps:

- Baseline comparison of various zigzag designs with different avalanche schemes
- Study impact of diffusion on resolution to see if it's worth increasing the pad pitch to further reduce channel count
- Survey of gas mixtures for different MPGDs
- Investigate possibility of providing 2D high resolution space points
- Examine the need for resolution over occupancy and vice-versa

10.2 R&D on cylindrical μRWELL Prototype for EIC Fast Tracking Layer

For the scenario where a TPC is chosen as the central tracker option for the EIC detector and MAPS technology is adopted for the vertex, we have identified three strong motivations for the need of a high-precision and fast-signal tracking detector to complement the inherent limitations of the TPC + MAPS as main tracking detectors in the barrel region.

- **High angular resolution tracking layer for the barrel PID detector:** As demonstrated by the studies shown on Fig. 17 of section 4.2.2, Micro resistive Well Detector (μRWELL) technology is able to provide the angular and space point resolutions requirements by DIRC detector in the barrel region to

achieve a 3σ π/K separation at 6 GeV. The simulation studies demonstrate that the 2 layers configuration surrounding the DIRC detector will vastly improve the PID detector performances.

- **High space point resolution tracking layer for TPC field distortions correction/calibration:** In addition to providing the angular resolution information to the DIRC detector, cylindrical μRWELL layers will also provide precision tracking to calibrate the TPC tracks and help correct for well known "scale distortions" of TPC tracks. For this case, the optimal configuration will be two cylindrical μRWELL layers, the first inside the TPC inner field cage and the second, outside. We are performing simulation studies for the two-layers configurations to evaluate the performances.
- **Fast tracking layer to complement slow TPC and MAPS detector** Both TPC and MAPS technologies are slow detectors and having an additional fast tracker with a timing resolution of a few ns will be required to provide the bunch crossing timing information to the reconstructed vertex as well as central tracks. μRWELL detector technologies provides the timing resolution needed to satisfy these requirements

The μRWELL is one of the novel MPGD technologies that would meet the requirements for low cost, large area, high precision and fast tracking layers. Florida Tech (FIT), Temple University (TU) and University of Virginia (UVa) as part of the eRD6 program have been investigating the possibility for large cylindrical μRWELL. Building upon the current ongoing μRWELL R&D activities among the three institutions, we propose a joint effort to build and characterize a fully functional small prototype cylindrical μRWELL detector. This will be the first time that a cylindrical μRWELL detector will be built and characterized.

10.2.1 μRWELL amplification & readout structure: UVa

The UVa group will be in charge of the overall design of the sensitive area of the cylindrical. In coordination with the colleagues from FIT and TU, we will design the μRWELL amplification layer, the drift cathode foil as well as readout plane. The diameter of cylindrical prototype will be approximately 20 cm with a total length of 55 cm. The FE electronics will be located at both edges of the cylinder as shown in Florida Tech mock-up design in section 5.2.1. The readout plane for the cylindrical μRWELL prototype will be based on the high performance large-pad capacitive-sharing readout scheme that is currently under development at UVa and described in subsection 4.4.3. We anticipate readout with a pad size somewhere between 1 to 2 cm^2. The fall back option to the large-pad readout will be the U-V strip readout already developed and tested with UVa planar large GEM prototype. Experts at CERN will be consulted for input before the final design and layout of the μRWELL structure and will manufacture the device. We envision to complete the phase of designing and fabrication of the μRWELL parts by spring 2021. This will be followed by the assembly into detector and preliminary tests jointly performed by the 3 institutes in the second half of FY21.

10.2.2 Electronics and DAQ: Temple U.

The TU group will be responsible for the electronics and DAQ system used to readout the prototype. Ideally we would like to use DREAM and VMM electronics to readout our prototype detector. UVa has already purchased VMM electronics suitable for 512 channels from the previous funding cycle. If available, we would borrow some DREAM electronics from our other eRD6 colleagues (BNL and Saclay). All other remaining detector channels will be equipped with APV25. We anticipate to have the electronics and DAQ in place by the time fabrication is completed and preliminary testing begins in the second half of FY21.

10.2.3 Mechanical Support Structure: Florida Tech

Building on its experience with designing and constructing the mechanical mock-up, the Florida Tech group plans to focus on developing the mechanics for the first functional cylindrical μRWELL prototype. Sealing the gas volume will be one of the critical technical issues to be addressed. The mock-up work shows that it is currently difficult to assemble the detector with the O-rings in place. The O-ring groove will have to

be optimized to precisely matched to the O-ring, which will require a redesign and leak testing. We will investigate what the most reliable way is for splicing the edges of the foils together to form continuous leak-tight cylinders. We will review the design and investigate the optimal material choice for the end-rings in light of the required precision. Given the simulation results on the material estimate for the current mock-up (Fig. 18), we will attempt to reduce material in the end-rings. This will depend on how much mechanical support they need to offer to the readout connectorizations that we will choose. For example, if they only need to support connectors and flex cables rather than full front-end boards, they could potentially be made thinner. The suspension of the cylindrical structure with nylon rods will be tested with respect to its long-term stability. We will use the existing mock-up in these studies, design and produce the mechanics for the functional prototype, and work with UVa on the final integration with the readout and drift foil.

10.3 R&D on EIC End Cap GEM Trackers

	Status of the prototype	Assembly technique	Readout technology	spatial resolution	Low mass	Dead area from support frames	Dead area in active area	FE cards connection
FIT FT-GEM 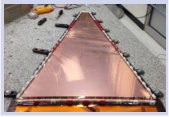	Assembled – Technical issues – Fixes underway (-)	**Mech. Stretching technique - chamber can be reopened** (+)	1D Zigzag strips (-)	100 µm (+) but 1D only	**Yes** (+)	Carbon Fiber, G10 Fiber glass, metallic piece (-)	**No spacers** (+)	Standard - Outside active area (+)
UVa FT-GEM 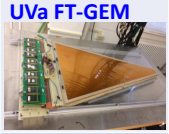	**Assembled – Tested in beam at FNAL** (+)	Glued frames - chamber can't be reopened (-)	**2D U-V stereo-angle strips** (+)	100 µm × 400 µm (+)	**Yes** (+)	**Fiber glass (G10) 15 mm** (+)	300 µm straight spacers grid (-)	**Zebra - Outside active area** (+)
TU FT-GEM 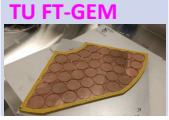	STAR FGT Technical issues – Fixes underway (-)	Glued frames - chamber can't be reopened (-)	**2D radial-Azimuth strips** (+)	**100 µm × 100 µm** (+)	**Yes** (+)	(G10) 15 mm but FE cards on side (-)	50 µm Kapton rings (-)	Outside active area But FE on side (-)?

Figure 26: Comparisons of the differences in assembly techniques and readout strip layer options of the three large GEM prototypes designed at UVa, FIT and TU as R&D for the forward tracker of an EIC detector.

Here, we present a brief introduction of the R&D effort conducted by three institutions, Florida Tech, University of Virginia, and Temple University to design, prototype and build, and characterize large area and lightweight triple-GEM detector prototypes for tracking in the end cap regions of an EIC detector. The R&D program was primarily focused on the development of large area and lightweight i.e. low mass triple-GEM chambers with the goal to minimize the multiple scattering that would affect the on the angular and momentum resolution performances specially for low energy electrons in the electron end cap for example. Large area trackers rather than tiles of smaller size modules allow a better optimization of dead-to-active area ratio. Each of the prototypes proposed by the three institutes is expected to meet these basic EIC tracking requirements. However there are some key differences between the technical options chosen by each institute to design and build its prototype. The assembly technique of these prototypes as well as the choice of the anode readout PCB layer technologies are among the differences between the 3 prototypes.The table shown on Fig.26 provides a brief summary of some of the main characteristics of each prototypes and the expected performances of the detectors and presents the pros and cons of each of the technological choices.

10.3.1 End Cap GEM Tracker with 2D U-V strips readout: UVA

The UVa prototype will be evaluated once again in test beam at Fermilab in Spring 2021 to finalize the spatial resolution studies and the overall characterisation of the prototype after a number of minor issues

identified during the first FNAL test beam in 2018 were addressed.

The generic R&D phase of large area and light-weight EIC End Cap GEM with 2D strip U-V readout will then be completed.

10.3.2 Carbon Fiber End Cap GEM Tracker: Florida Tech

We are redesigning the inner frames of the detector assembly to strengthen them for better taking up the forces exerted by the stretching screws and nuts. Compared with the existing frames (Fig. 20), the stretching screw and nuts will have a more snug fit in the cutout in the new design (Fig. 27). The arches in the frames are eliminated in favor of a new straight and wider design (Fig. 27). The current inner frame pieces are a mix of stronger PEEK and weaker ABS materials. In the refurbished detector, the entire inner frame stack will be made from PEEK. The frame pieces will be cut from PEEK plates using a water jet in the university machine shop.

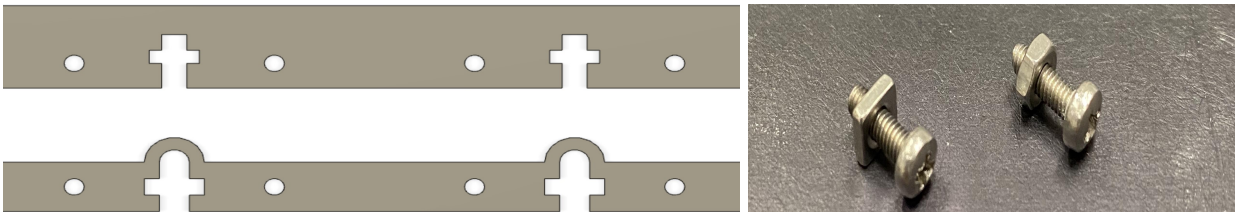

Figure 27: Redesign of inner frames of large carbon fiber GEM prototype. Left: New inner frame piece (top) with longer tabs in cutout and without arches compared with current frame piece (bottom). Right: Square nut vs. hex nut with stretching screw.

If these final refurbishments are successful in eliminating shorts between foils due to improved stretching, we will perform a full set of quality control tests on the refurbished low-mass prototype and characterize its performance, e.g. gain curves, with X-rays at Fl. Tech.

On the simulation side, we will use the new Fun4all simulation environment to study track-hit residuals of forward tracks as a function of central tracker and forward tracker material. A new Ph.D. student, Merrick Lavinsky, has joint the effort and will take on this task.

10.4 R&D on EIC RICH Detectors

The RICH counter for high momentum hadrons required at EIC in the forward region represents a challenge because, due to the limited space available, the presence of the magnetic field and the restrictions on the total material budget, a complete conceptual design of this detector is not yet possible. The activity dedicated to particle PID within eRD6 is focused to investigate key issues related to this counter with the goal of making its design feasible and solid. The main open questions related to the design of the forward RICH are listed in the following with reference to the corresponding R&D studies ongoing within eRD6.

The choice of the radiator gas Standard fluorocarbons are selected because of their limited chromaticity. Nevertheless, the environmental impact of their use related to attacking ozone and, even more dramatic, their high GWP is imposing restrictions on their use in an increasing number of countries around the world, also impacting on the procurement options and the cost. The chromatic figures of noble gasses are favorable, while their low density at atmospheric pressure limits the Cherenkov photon rates. A possible alternative is the use of noble gasses at high pressure. For example, Ar at P = 3 bar mimics C_2F_6 for what concerns chromatic characteristics and Cherenkov photon rate. The use of a pressurized vessel has implications in mechanical design, photon detector interfaces and gaseous photon detector operation. The eRD6 activity reported in Appendix B is related to this option.

A fully innovative alternative is the use of radiators by meta-materials specifically designed to mimic by solid state components the Cherenkov effect in gasses. The eRD6 activity reported in Sec. 6.2.4 is dedicated to these studies.

The optical configuration Two basic schemes can be considered. In central reflection configurations, the photon detectors are centered on the mirror axis, therefore they are sitting in the detector acceptance region. This arrangement provides the minimum spherical aberration. At the same time, the detector material is part of the overall material budget and very light gaseous photon detectors are required. Moreover, these detectors are challenged by the particle rates present in the acceptance region and they have to be operated at high pressure if the pressurized radiator gas option is adopted. These detectors are studied in Appendix B, Appendix D.2 and Sec. 6.4.1. In non-central reflection configurations, double or triple reflections are required and, therefore, the photon detectors can sit outside the acceptance region, relaxing the requirements about the their material budget and their rate capabilities. Nevertheless, the non-central optical alignment introduces important image distortions due to spherical aberration, reducing the maximum particle momentum at which hadron identification is effective. In all the different design schemes, high quality mirrors are needed, that need to reflect in the far UV domain, when gaseous photon detectors are used. Mirror developments are reported in Sec. 6.2.3.

Adequate photon detectors The use of detectors of the PMT family is excluded due to the presence of a magnetic field. MCP-based detectors can be considered, even if their correct operation is subject to verification according to the details of the magnetic field configuration. The ones presently available from industry are extremely expensive, while the LAPPDs are still under development, in particular the version generation 3, which is the most adequate version, thanks to the compatibility with a pad read-out. These photon detectors can be of interest also for PID counters at low and intermediate momentum. In this context, gaseous detectors and their readout based on MPGD technologies represent a concrete option and they are intensively developed within eRD6: Appendix A, Appendix B, Appendix D.2 and Sec. 6.4.1. Moreover, the possibility to replace CsI photocathodes, the only one coupled to gaseous photon detectors so far, with more robust and chemically more stable photoconverters based on hydrogenated nano-diamond power is being explored as an alternative to CsI: Sec. 6.4.2.

11 eRD6 Budget Request for FY21

11.1 Overall Budget Request and Money Matrix

The institutional budget requests presented below are summarized in the following. The overall money matrix of R&D project vs. Institute for the eRD6 funding requests for FY21 is presented in Table 1

Table 1: Fully loaded cost matrix of institutes and R&D topic for the eRD6 FY21 budgetary request

k$	**μRWELL Cyl. Layer**	**Micromegas Barrel Tracker**	**TPC Readout**	**Forward Tracker**	**MPGD RICH**	**High Press. RICH**	**Total**
BNL & Yale U.			79.5				**79.5**
Florida Tech	46.19			3.49			**49.68**
INFN Trieste					38		**38**
Temple U.	33.5						**33.5**
CEA Saclay		8					**8**
SBU						24.15	**24.15**
UVa	50						**50**
Total	**129.69**	**8**	**79.5**	**3.49**	**38**	**24.15**	**282.83**

11.2 Budget Request by Institute

11.2.1 BNL Budget Request for FY21

Our budget request for this funding cycle will mainly consist of the continued development of readout structures optimized for a TPC. A portion of this focus will go to applying our existing concepts for interleaved anode structures to PID applications, including LAPPDs, mRICH, and MCP-PMTs. For the TPC work, an appropriate anode pattern must be paired with a given avalanche scheme and working gas combination, which requires the procurement of several new readout PCBs. While the work on PID readouts will capitalize on many existing resources used for developing interleaved readout designs in general, it will entail the procurement of additional PCBs for testing. The R&D plans described here also include a beam test in the Spring of 2021, which will require preparation beforehand. Finally, it must be reiterated that this budget request is to be shared with the Yale group since they will collaborate on much of this work.

Table 2: Budget request for TPC R&D at BNL and Yale ,including 20% and 40% reduction scenarios (FY21)

	Baseline (k$)	**-20% (k$)**	**-40% (k$)**
TPC interleaved readout boards	15	12	9
TPC avalanche structures (Micromegas, μRWELL)	5	4	3
PID interleaved readout boards	10	8	6
Technical support	12	9.6	7.2
Gas and other expendables	6	4.8	3.6
Travel	5	4	3
Total	53	42.4	31.8
Overhead	26.5	21.2	15.9
Total with overhead	**79.5**	**63.6**	**47.7**

11.2.2 Florida Tech Budget Request for FY21

We request funding to cover stipends for two graduate students, Jerry Collins and Merrick Lavinsky, and a stipend for two undergraduate summer students. Collins has produced the design of the cylindrical μRWELL system and constructed the mechanical mock-up. Lavinsky joined in summer 2020 and has begun work on GEANT4 and fun4all simulations of tracking in the forward region. We also request travel funds for the P.I. to attend an EIC R&D review meeting and funds for travel for integrating the components of the cylindrical μRWELL system and testing. Funds are requested for procuring and machining materials for the mechanics of the functional cylindrical μRWELL prototype.

Table 3 breaks down the funding request for the Florida Tech projects, along with the 20% and 40% reduced funding scenarios. In the 20% reduced scenario, we mainly drop support for the undergraduate summer students and reduce travel. In the 40% reduced scenario, graduate student support for summer 2021 is cut in half, and travel is much reduced. Florida Tech does not charge benefits or overhead on students for the current grant.

Table 3: **Florida Tech** - FY21 budget request including scenarios with 20% and 40% reduction.

	Request	**-20%**	**-40%**
Graduate Student Stipends (2 stud.)	\$27,400	\$26,400	\$21,816
Undergraduate Summer Stipend	\$6,000	\$0	\$0
Travel	\$6,000	\$4,000	\$1,400
Materials	\$5,000	\$5,000	\$4,000
Indirect Cost Base (travel & material)	\$11,000	\$9,000	\$5,400
Indirect Cost (48% negotiated rate)	\$5,280	\$4,320	\$2,592
Total	**\$49,680**	**\$39,720**	**\$29,808**

11.2.3 INFN Budget Request for FY21

The 2021 activity consists in the continuation of the two tasks already pursued in 2018, 2019 and 2020 and detailed in Secs. 6.4.1 and 6.4.2. A non negligible fraction of this activity includes items that could not be performed in 2020 due to the pandemic emergency and the related shutdown. Therefore, **the 2021 request does not include consumables for those items already financed for 2020**. Also, **it includes very limited requests for travelling as this can be covered by the unused 2020 resources**.

The resulting founding request for this R&D activity, 38 k\$ in total, includes three main chapters:

1. the financial support for a postdoc (7 months) fully dedicated to the project: the contribution of a dedicated personnel unit will offer a crucial boost to the R&D program; this support will be complemented by INFN resources in order to result in one full-year postdoc contract dedicated to the project;
2. the required traveling resources, mainly to have the possibility of closer interaction with the whole eRD6 Consortium and to follow the evolution of the EIC project: two trips to US require about 6000 \$; a minor support is requested to allow travelling to and from Bari and Trieste for the common work about the ND photocathodes: this needs is estimated to be 2000 \$; another minor support is requested for material procurement, to interact with the producers when non-standard components are needed and for the construction of specific detector elements that must be produced at CERN: this needs is estimated to be 2000 \$; part of this needs will be covered by the unspended 2020 money and, therefore, the request for 2021 is limited to of 5000 \$;
3. Consumables are request only for one of the novel items of the activity planning, namely the complete small size prototype of photon detector with photocathode by hydrogenated nanodiamond powder and for operational costs. Consumables for FY2021 include:

- Material and fabrication of complete small size prototype of photon detector with photocathode by hydrogenated nanodiamond powder: 6000 $;
- Miscellanea of laboratory small items: 2000 $.

Cost reductions in -20% and -40% scenarios
The requests have been carefully analyzed and kept at a minimal level. Any reduction would severely impact. In the "-20%" hypothesis one of the two foreseen activity has to be stopped. In the "-40%" hypothesis the whole INFN Trieste activity will be stopped.

The requests are summarized in Table 4.

Table 4: Funding request INFN

item	cost (k$)	overhead (k$)	total (=cost+overhead) (k$)
manpower	20	4	24
traveling	5	1	6
consumables	8		8
total	33	5	38

11.2.4 CEA Saclay Budget Request for FY21

In the context of eRD6, we will focus its effort on the studies of a barrel cylindrical Micromegas solution for an EIC detector. In this context the detector simulations will be carried out mainly by two post-doctoral researchers whose related fundings have been already secured. The simulations results will also allow us to collaborate with the other eRD6 groups and with the EIC Yellow Report tracking working group.

The studies on the readout solutions for the curved Micromegas tiles are already the subject of investigation of PhD students (not eRD6 funded) and it will further benefit of the collaboration with the eRD6 groups already involved in similar topics for other technological solutions. In particular, CEA-Saclay funding request will be dedicated to the testing of the new large pad readout PCB concept developed by UVa, see Appendix D.1, but with a Micromegas amplification stage.

In this context, CEA-Saclay plans to obtain one PCB board and to bulk a Micromegas on top of it, to test this device with the in house muon telescope and to test it during the test beam at Fermilab.

Table 5: R&D at CEA-Saclay (FY21)

	Baseline (k$)	**-20% (k$)**	**-40% (k$)**
Large pad readout board	4	3.2	2.4
Travel	4	3.2	2.4
Total with overhead	**8**	**6.4**	**4.8**

11.2.5 SBU Budget Request for FY21

We are requesting funding for the activities in FY21 as described in Appendix B.
We are requesting funding for upgrading our RICH-prototype. This concerns mainly the accommodation of high-pressure withstanding end-caps, around the MPGD-readout stage and the mirror. Furthermore, we will need to acquire a compressor system plus control system for obtaining the required pressure for the radiator.

We are requesting funding for acquiring a PCB as described in Appendix D.2.
We are requesting funding for acquiring standard 10×10 cm^2 GEMs but with specialized photo-cathode patterns.
The funding requests including a minus 20% as well a minus 40% funding scenario are summarized in Tab. 6. It should be noted that the decreased funding requests would lead to the cancellation of various activities.

Table 6: Funding request from **SBU** for FY21. The table includes scenarios with 20% and 40% reduction.

	Request	**-20%**	**-40%**
Transfer pads readout board	$ 3,000	N/A	N/A
GEMs	$ 1,200	$ 1,200	N/A
Compressor-/control-system	$ 7,750	$ 7,750	$ 7,750
Travel (incl. IDC)	$ 4,650	$ 2,820	N/A
Materials (incl. IDC)	$ 7,550	$ 7,550	$ 6,740
Total	$ **24,150**	$ **19,320**	$ **14,490**

11.2.6 TU Budget Request for FY21

For this funding cycle the majority of our request would be the partial support of a postdoc who would work on the planar μRWell μTPC detector and the cylindrical μRWell detector. Some material money is requested for HV boards, cables, gas, etc. A more detailed description of our FY21 plans are below, and Table 7 summarizes our FY21 funding request.

Table 7: TU funding request for FY21 with 20% and 40% reduction scenarios.

Item	Request ($)	-20% ($)	-40% ($)
Postdoc (%)	(20%) 11,274	(15%) 8,455	(15%) 8,455
Fringe benefits (25.5%)	2,875	2,156	2,156
Total Personnel	14,148	10,611	10,611
Material	1,000	1,000	1,000
Travel (Domestic)	6,000	4,000	2,000
Total Direct Costs	21,148	15,611	13,611
Modified Total Direct Costs	21,148	15,611	13,611
Overhead (58.5%)	12,523	9,133	7,963
Total Project Costs	**33,520**	**24,744**	**21,574**

1. Assemble and characterize a planar 10 cm × 10 cm μRWELL from CERN operating in μTPC mode with a drift gap of 15 mm.

2. Continue developing μRWELL detector simulation in collaboration with FIT and UVa.

3. In collaboration with FIT and UVa colleagues, we plan to design and build a small cylindrical μRWELL. TU would be responsible for equipping the detector electronics and DAQ.

4. Support for a partial postdoc who would work on characterizing the 10 cm × 10 cm planar μRWELL operating in μTPC mode and equipping the cylindrical μRWELL prototype electronics and DAQ.

5. Travel money is being requested in order to attend the EIC *R&D* review meetings and to fund travel for integrating the components of the cylindrical μRWELL system and testing.

11.2.7 UVa Budget Request for FY21

For this funding cycle, the bulk of UVa budget request will concentrate on the development new large pad readout PCBs with μRWELL amplification device. We plan is to:

1. First, establish the proof of concept of the new large pad readout PCB with a μRWELL technology on a small standard form factor prototype.
2. Investigate ways to minimize capacitance noise and cross talk effects of large pad readout by testing various pad patterns designs on one single large readout PCB with triple-GEM amplification.
3. In collaboration with Florida Tech. and Temple U colleagues, we plan to design and build a small cylindrical μRWELL. Our group at UVa is in charge of the design, layout and production of the μRWELL device with an approximate area of 60 cm $\times$ 50 cm with the new large-pad readout PCB.
4. We plan to request support funding for undergrad student stipends to work μRWELL detector development and characterization and participating in test beam data at FNAL and the subsequent analysis

The table below 8 summarize the breakdown of UVa funding request for FY21 cycle.

Table 8: UVa FY21 budget request with 20% and 40% reduction scenario

Item	**Budget Request**	**-20% scenario**	**-40% scenario**
R&D on μRWELL with Large-Pad Readout	\$5,000	\$3,000	\$3.000
R&D on Large-Pad & Low Capacitance Readout	\$5,000	\$3,000	\$0,000
Design and fabrication of cylindrical μRWELL	\$15,000	\$15,000	\$15,000
Lab Supplies & Expendables	\$3,000	\$2,000	\$1,000
Travel (fully loaded)	\$9,000	\$6,000	\$4,000
Undergraduate Stipend	\$3,000	\$2,400	\$1,800
Undergraduate Summer Stipend	\$6,000	\$4,800	\$3,600
Overhead (61%)	\$4,000	\$3,000	\$2,000
Total	**\$50,000**	**\$39,200**	**\$30,400**

12 List of all EIC publications from the eRD6 Consortium

BNL publications:

[1] B. Azmoun et al. "Design Studies of High Resolution Readout Planes using Zigzags with GEM Detectors". In: *IEEE Transactions on Nuclear Science* PP (June 2020), pp. 1–1. DOI: 10.1109/TNS.2020.3001847.

[2] B. Azmoun et al. "Results From a Prototype Combination TPC Cherenkov Detector With GEM Readout". In: *IEEE Transactions on Nuclear Science* 66.8 (Aug. 2019), pp. 1984–1992. ISSN: 1558-1578. DOI: 10.1109/TNS.2019.2928269.

[3] B. Azmoun et al. "Design Studies for a TPC Readout Plane Using Zigzag Patterns with Multistage GEM Detectors". In: *IEEE Transactions on Nuclear Science* (July 2018), pp. 1–1. ISSN: 0018-9499. DOI: 10.1109/TNS.2018.2846403.

[4] B. Azmoun et al. "A Study of a Mini-Drift GEM Tracking Detector". In: *IEEE Transactions on Nuclear Science* 63.3 (June 2016), pp. 1768–1776. ISSN: 0018-9499. DOI: 10.1109/TNS.2016.2550503.

[5] Craig Woody et al. "A Prototype Combination TPC Cherenkov Detector with GEM Readout for Tracking and Particle Identification and its Potential Use at an Electron Ion Collider". In: 2015. arXiv: 1512.05309 [physics.ins-det]. URL: https://inspirehep.net/record/1409973/files/arXiv:1512.05309.pdf.

[6] B. Azmoun et al. "Initial studies of a short drift GEM tracking detector". In: *2014 IEEE Nuclear Science Symposium and Medical Imaging Conference (NSS/MIC)*. Nov. 2014, pp. 1–2. DOI: 10.1109/NSSMIC.2014.7431059.

[7] M. L. Purschke et al. "Test beam study of a short drift GEM tracking detector". In: *2013 IEEE Nuclear Science Symposium and Medical Imaging Conference (2013 NSS/MIC)*. Oct. 2013, pp. 1–4. DOI: 10.1109/NSSMIC.2013.6829463.

Florida Tech publications:

[1] Marcus Hohlmann et al. "Low-mass GEM detector with radial zigzag readout strips for forward tracking at the EIC". In: *2017 IEEE Nuclear Science Symposium and Medical Imaging Conference (NSS/MIC 2017) Atlanta, Georgia, USA, October 21-28, 2017*. 2017. arXiv: 1711.05333 [physics.ins-det]. URL: http://inspirehep.net/record/1636290/files/arXiv:1711.05333.pdf.

[2] Aiwu Zhang et al. "A GEM readout with radial zigzag strips and linear charge-sharing response". In: *Nucl. Instrum. Meth.* A887 (2018), pp. 184–192. arXiv: 1708.07931 [physics.ins-det].

[3] Aiwu Zhang and Marcus Hohlmann. "Accuracy of the geometric-mean method for determining spatial resolutions of tracking detectors in the presence of multiple Coulomb scattering". In: *JINST* 11.06 (2016), P06012. DOI: 10.1088/1748-0221/11/06/P06012. arXiv: 1604.06130 [physics.data-an].

[4] Aiwu Zhang et al. "R&D on GEM detectors for forward tracking at a future Electron-Ion Collider". In: *Proceedings, 2015 IEEE Nuclear Science Symposium and Medical Imaging Conference (NSS/MIC 2015): San Diego, California, United States*. 2016, p. 7581965. DOI: 10.1109/NSSMIC.2015.7581965. arXiv: 1511.07913 [physics.ins-det]. URL: http://inspirehep.net/record/1406551/files/arXiv:1511.07913.pdf.

[5] Aiwu Zhang et al. "Performance of a Large-area GEM Detector Read Out with Wide Radial Zigzag Strips". In: *Nucl. Instrum. Meth.* A811 (2016), pp. 30–41. DOI: 10.1016/j.nima.2015.11.157. arXiv: 1508.07046 [physics.ins-det].

INFN publications:

[1] J. Agarwala et al. "The MPGD-based photon detectors for the upgrade of COMPASS RICH-1 and beyond". In: *Nuclear Instruments and Methods in Physics Research Section A: Accelerators, Spectrometers, Detectors and Associated Equipment* (2018). ISSN: 0168-9002. DOI: https://doi.org/10.1016/j.nima.2018.10.092. URL: http://www.sciencedirect.com/science/article/pii/S0168900218314062.

[2] J. Agarwala et al. "Study of MicroPattern Gaseous detectors with novel nanodiamond based photocathodes for single photon detection in EIC RICH". In: *Nuclear Instruments and Methods in Physics Research Section A: Accelerators, Spectrometers, Detectors and Associated Equipment* (2019). ISSN: 0168-9002. DOI: https://doi.org/10.1016/j.nima.2019.03.022. URL: http://www.sciencedirect.com/science/article/pii/S0168900219303213.

[3] J. Agarwala et al. "Optimized MPGD-based Photon Detectors for high momentum particle identification at the Electron-Ion Collider". In: *Nuclear Instruments and Methods in Physics Research Section A: Accelerators, Spectrometers, Detectors and Associated Equipment* 936 (2019). Frontier Detectors for Frontier Physics: 14th Pisa Meeting on Advanced Detectors, pp. 565–567. ISSN: 0168-9002. DOI: https://doi.org/10.1016/j.nima.2018.10.185. URL: http://www.sciencedirect.com/science/article/pii/S0168900218314992.

[4] J. Agarwala et al. "A modular mini-pad photon detector prototype for RICH application at the Electron Ion Collider". In: *Journal of Physics: Conference Series* 1498 (Apr. 2020), p. 012007. DOI: 10.1088/1742-6596/1498/1/012007. URL: https://doi.org/10.1088%2F1742-6596%2F1498%2F1%2F012007.

[5] C. Chatterjee et al. "Nanodiamond photocathodes for MPGD-based single photon detectors at future EIC". In: *Journal of Physics: Conference Series* 1498 (Apr. 2020), p. 012008. DOI: 10.1088/1742-6596/1498/1/012008. URL: https://doi.org/10.1088%2F1742-6596%2F1498%2F1%2F012008.

[6] J. Agarwala et al. *MPGD-based photon detectors for the upgrade of COMPASS RICH-1 and beyond.* 2020. arXiv: 2006.10447 [physics.ins-det].

[7] F. M. Brunbauer et al. *Nanodiamond photocathodes for MPGD-based single photon detectors at future EIC.* 2020. arXiv: 2006.02352 [physics.ins-det].

SBU publications:

[1] M. Blatnik et al. "Performance of a Quintuple-GEM Based RICH Detector Prototype". In: *IEEE Trans. Nucl. Sci.* 62.6 (2015), pp. 3256–3264. DOI: 10.1109/TNS.2015.2487999. arXiv: 1501.03530 [physics.ins-det].

TU publications:

[1] M. Posik and B. Surrow. "Construction of a Triple-GEM Detector Using Commercially Manufactured Large GEM Foils". In: 2018. arXiv: 1806.01892 [physics.ins-det].

[2] M. Posik and B. Surrow. "Construction of Triple-GEM Detectors Using Commercially Manufactured Large GEM Foils". In: *Proceedings, 2016 IEEE Nuclear Science Symposium and Medical Imaging Conference: NSS/MIC 2016: Strasbourg, France.* 2016, p. 8069743. DOI: 10.1109/NSSMIC.2016.8069743. arXiv: 1612.03776 [physics.ins-det].

[3] M. Posik and B. Surrow. "Optical and electrical performance of commercially manufactured large GEM foils". In: *Nucl. Instrum. Meth.* A802 (2015), pp. 10–15. DOI: 10.1016/j.nima.2015.08.048. arXiv: 1506.03652 [physics.ins-det].

[4] M. Posik and B. Surrow. "R&D of commercially manufactured large GEM foils". In: *Proceedings, 2015 IEEE Nuclear Science Symposium and Medical Imaging Conference (NSS/MIC 2015): San Diego, California, United States*. 2016, p. 7581802. DOI: 10.1109/NSSMIC.2015.7581802. arXiv: 1511.08693 [physics.ins-det].

[5] M. Posik and B. Surrow. "Research and Development of Commercially Manufactured Large GEM Foils". In: *Proceedings, 21st Symposium on Room-Temperature Semiconductor X-ray and Gamma-ray Detectors (RTSD 2014): Seattle, WA, USA, November 8-15, 2014*. 2016, p. 7431060. DOI: 10.1109/NSSMIC.2014.7431060. arXiv: 1411.7243 [physics.ins-det].

UVa publications:

[1] Kondo Gnanvo et al. "Large Size GEM for Super Bigbite Spectrometer (SBS) Polarimeter for Hall A 12 GeV program at JLab". In: *Nucl. Instrum. Meth.* A782 (2015), pp. 77–86. DOI: 10.1016/j.nima.2015.02.017. arXiv: 1409.5393 [physics.ins-det].

[2] Kondo Gnanvo et al. "Performance in test beam of a large-area and light-weight GEM detector with 2D stereo-angle (UV) strip readout". In: *Nucl. Instrum. Meth.* A808 (2016), pp. 83–92. DOI: 10.1016/j.nima.2015.11.071. arXiv: 1509.03875 [physics.ins-det].

Yale publications:

[1] S. Aiola et al. "Combination of two Gas Electron Multipliers and a Micromegas as gain elements for a time projection chamber". In: *Nucl. Instrum. Meth.* A834 (2016), pp. 149–157. DOI: 10.1016/j.nima.2016.08.007. arXiv: 1603.08473 [physics.ins-det].

References

[1] http://skipper.physics.sunysb.edu/~prakhar/tpc/HTML_Gating_RANDd/wires.html.

[2] J. Agarwala et al. "The MPGD-based photon detectors for the upgrade of COMPASS RICH-1 and beyond". In: *Nuclear Instruments and Methods in Physics Research Section A: Accelerators, Spectrometers, Detectors and Associated Equipment* (2018). ISSN: 0168-9002. DOI: https://doi.org/10.1016/j.nima.2018.10.092. URL: http://www.sciencedirect.com/science/article/pii/S0168900218314062.

[3] T. Kawamoto et al. "New Small Wheel Technical Design Report". In: (June 2013).

[4] M. Blatnik et al. "Performance of a Quintuple-GEM Based RICH Detector Prototype". In: *IEEE Transactions on Nuclear Science* 62.6 (2015), pp. 3256–3264.

[5] S. Aiola et al. "Combination of two Gas Electron Multipliers and a Micromegas as gain elements for a time projection chamber". In: *Nuclear Instruments and Methods in Physics Research Section A: Accelerators, Spectrometers, Detectors and Associated Equipment* 834 (2016), pp. 149–157. ISSN: 0168-9002. DOI: https://doi.org/10.1016/j.nima.2016.08.007. URL: http://www.sciencedirect.com/science/article/pii/S0168900216308221.

[6] Luciano Velardi, Antonio Valentini, and Grazia Cicala. "UV photocathodes based on nanodiamond particles: Effect of carbon hybridization on the efficiency". In: *Diamond and Related Materials* 76.Supplement C (2017), pp. 1–8. ISSN: 0925-9635. DOI: https://doi.org/10.1016/j.diamond.2017.03.017. URL: http://www.sciencedirect.com/science/article/pii/S0925963516306999.

[7] A. Bideau-Mehu et al. "Measurement of refractive indices of neon, argon, krypton and xenon in the 253.7-140.4 nm wavelength range. Dispersion relations and estimated oscillator strengths of the resonance lines." In: *J. Quant. Spectrosc. Rad. Transfer* 25 (1981), pp. 349–402. DOI: 10.1016/0022-4073(81)90057-1.

[8] A. Kramida et al. NIST Atomic Spectra Database (ver. 5.7.1), [Online]. Available: `https://physics.nist.gov/asd` [2017, April 9]. National Institute of Standards and Technology, Gaithersburg, MD. 2019.

[9] M. Blatnik et al. "Performance of a Quintuple-GEM Based RICH Detector Prototype". In: *IEEE Trans. Nucl. Sci.* 62.6 (2015), pp. 3256–3264. DOI: 10.1109/TNS.2015.2487999. arXiv: 1501.03530 [physics.ins-det].

[10] A. Bondar, A. Buzulutskov, and Lev I. Shekhtman. "High pressure operation of the triple-gem detector in pure ne, ar and xe". In: *Nucl. Instrum. Meth. A* 481 (2002), p. 200. DOI: 10.1016/S0168-9002(01)01369-9. arXiv: physics/0103082.

Appendices

A Appendix: MPGD sensors of single photons

Here, we present a brief introduction to two items related to INFN activity within eRD6, namely the principle and architecture of the MPGD sensors of single photons and the developments of new photocathode materials suitable for gaseous photon detectors.

A.1 The principle and architecture of the MPGD sensors of single photons and the related R&D

The concept of the hybrid MPGD detector of single photons has been developed in an eight-year R&D program; the requirements for the upgrade of the gaseous RICH counter of the COMPASS experiment at CERN SPS are the reference that guided this development. The resulting detectors have been successfully in operation at COMPASS since Spring 2016 [2]. The detector architecture (Fig. 28) consists in three multiplication stages: two THick GEMs (THGEM) layers, the first one coated with a CsI film and acting as photocathode, followed by a MicroMegas (MM) multiplication stage. The two THGEMs are staggered: this configuration is beneficial both to reduce the Ion BackFlow (IBF) and to increase the maximum gain at which the detector can be operated exhibiting full electrical stability. These photon detectors are routinely operated at gains of 1.5×10^4 and exhibit an IBF rate lower than 3%. The gas mixtures used are by Ar and CH_4, with a rich methane fraction in order to maximize the photoelectron extraction. An original element of the hybrid MPGD photon detector is the approach to a resistive MM by discrete elements (Figure 29), which has been triggered by the resistive MM developed for the ATLAS experiment at CERN LHC [3], even if there are substantial differences. The anode elements (pads) facing the micromesh are individually equipped with large-value resistors and the HV is provided, via these resistors, to the anode electrodes, while the micromesh is grounded. A second set of electrodes (pads parallel to the first ones) are embedded in the anode PCB: the signal is transferred by capacitive coupling to these electrodes, which are connected to the front-end read-out electronics. The advantages of the design shortly described above are several:

- As in ATLAS resistive MM, applying the HV to the anode instead of to the MM cathode results in

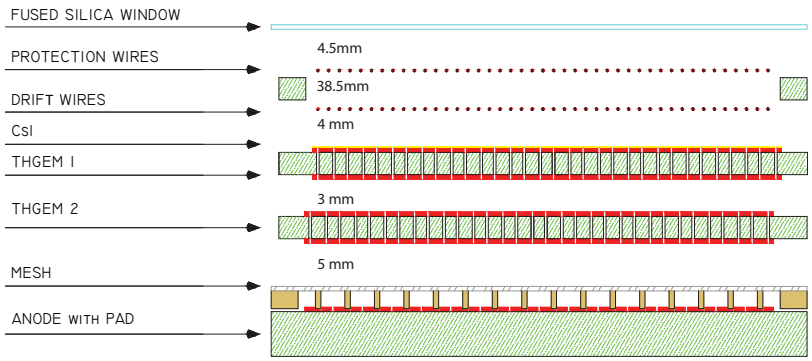

Figure 28: Sketch of the hybrid single photon detector: two staggered THGEM layers are coupled to a resistive bulk MM. Image not to scale.

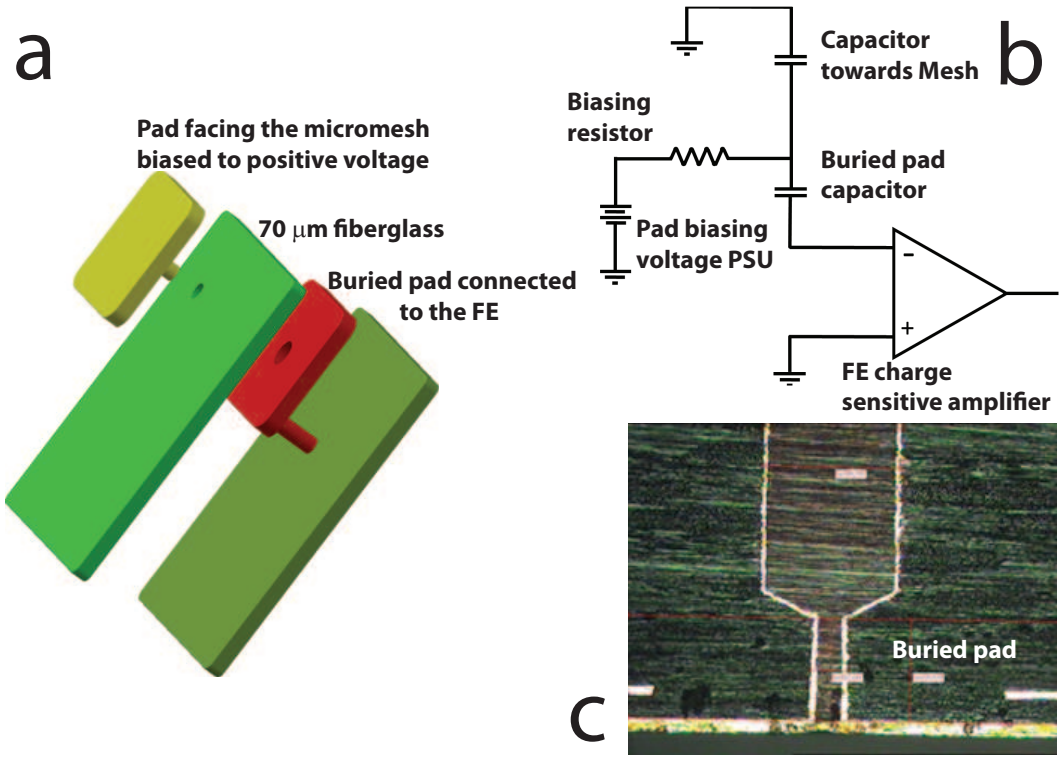

Figure 29: a) Sketch of the capacitive coupled readout pad. The biasing voltage is distributed via independent 470 MΩ resistors to the pad facing the micromesh structure (yellow pad in the sketch). The buried pad (red pad in the sketch) is isolated via 70 μm thick fiberglass and connected to the front end chip. b) Schematic of the capacitive coupled pad principle illustrated via discrete element blocks. c) Metallography section of the PCB: detail of the through-via connecting the external pad through the hole of the buried pad. The reduced diameter of the through-via reaching the external pad contributes preserving the pad planarity.

larger amplitude signals;

- In case of local defects of the MM, a single electrode can be isolated resulting in a dead area as large as the electrode itself, while the large majority of the detector is still active;
- No resistive coating is present inside the detector volume;
- The absence of a resistive layer on top of the anode electrodes is limiting the degradation of the dE/dx information in the collected signals.

The hybrid detector concept can be further improved in order to match the requirements of high momenta hadron identification at EIC; this challenging task requires:

1. Limited radiator length of the order of 1 m: here one of the most promising approaches is the windowless RICH concept [4];
2. Fine space granularity to cope with the modest lever arm related to the radiator length;
3. Control of the IBF rate in order to guarantee stable detector performance over time;
4. Further improvement in the engineering aspects in order to improve the detector robustness, simplify the construction and control the costs;

5. The comparison between hybrid detectors where THGEMs or GEMS in view of an overall optimization of the detector principle;

6. the identification and validation of an appropriate front-end ASIC for the use of these photon detectors in ten years from now.

The R&D program has progressed with the goal of matching the requirements listed above, while a summary of the performed activity is listed in the following.

- Test of novel materials for THGEM substrate to simplify the detector construction, increase the yield of valid large-size THGEMs and, thus, control the detector costs *(related to requirement 4)*;
- The development of resistive MM by discrete elements with miniaturized pad size in order to obtain finer space resolution *(related to requirement 1)*; a prototype has been built (Fig. 30), characterized by laboratory exercises and at a test beam data taking, where Cherenkov photons have been detected (Fig. 31); a dedicated DAQ system has been developed for the test beam studies, designed to increase the data bandwidth from the SRS read-out; a second version of the prototype aimed at improving its performance has been designed and it is ready for construction;
- The VMM3 ASIC is a novel chip designed for MPGDs with features promising for our application. In fact, the low noise figure and the capability of effective coupling with detectors in a wide capacity range are specifically beneficial to our single photon detection application, namely an application requiring single photoelectron detection, performed by a hybrid MPGD where the last multiplication stage is by a MICROMEGAS, namely a relatively high capacitance detector. Moreover, the chip architecture is designed for trigger-less operation, namely adequate for usage in up-to-date DAQ systems. We have acquired two pieces of the MMFE1 board, a VMM read-out board developed in the context of the ATLAS NSW project, design to exploit all the most relevant VMM3 features, including the good noise figures. In parallel, we have designed a dedicated MICROMEGAS prototype, designed according to our architecture of resistive micromegas changing the connectors so that part of the detector can be read with the MMFE1 board and part using an SRS-APV25 card in comparative exercises The PCB design is now ready for submission. This activity is *related to requirement 6*.

It is relevant to underline that the further development of the hybrid detector concept, in particular low IBF rate is **synergic** to another sector of activities within eRD6, namely the **read-out sensors for the TPC**. A hybrid MPGD approach to TPC read-out has already been proposed making use of traditional non-resistive MMs[5]; our approach to resistive MM can offer a detector which exhibits robust electrical stability while preserving a good dE/dx resolution.

A.2 The developments of new photocathode materials suitable for gaseous photon detectors

This activity consists in initial studies to understand the compatibility of an innovative photocathode material with the operation of gaseous detectors as well as in progressing in the characterization of the photoconverter itself.

The option of using innovative photoconverters in gaseous detectors is a strategic one. In fact, so far, the only photoconverter compatible with large-size, operative gaseous detector is CsI. Despite remarkable successful applications (for instance the read-out sensors of the ALICE RICH, the COMPASS RICH and the PHENIX HBD), the use of CsI in gaseous detector suffers from some intrinsic limitations: ageing, causing a severe decrease of the quantum efficiency after a collected charge of the order of some mC/cm^2 and long recovery time (about 1 day) after an occasional discharge in the detector. These limitations are related to the photon feedback from the multiplication region and to the bombardment of the CsI photocathode film by positive ions generated in the multiplication process. They impose to operate the detector at low gain, reducing the efficiency of single photoelectron detection. Alternatively, great care is required to reduce photon feedback

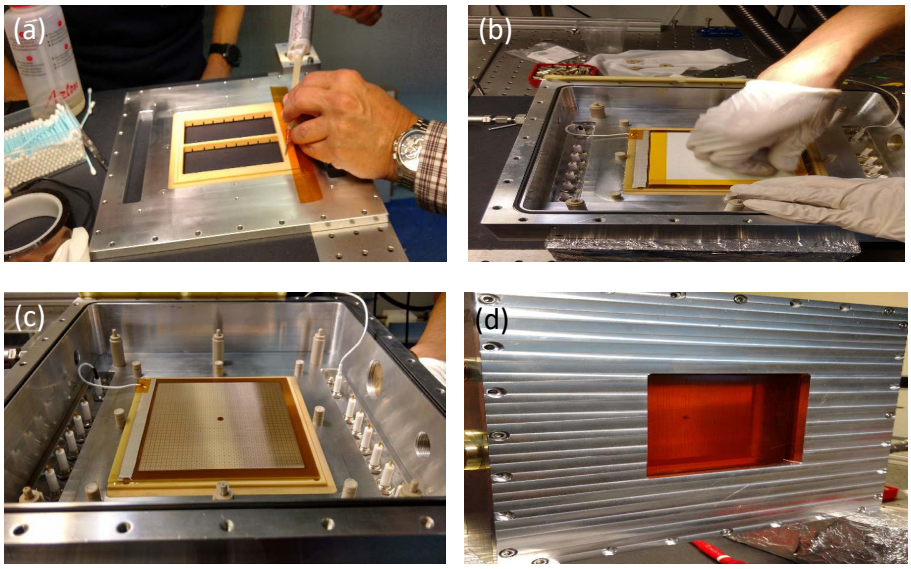

Figure 30: Prototype construction. (a) The fiberglass frame supporting the MM is glued onto the Al chamber structure. (b) The MM is glued onto the fiberglass frame. (c) The MM installed in the chamber and its power lines are visible. (d) The chamber is closed with a mylar window.

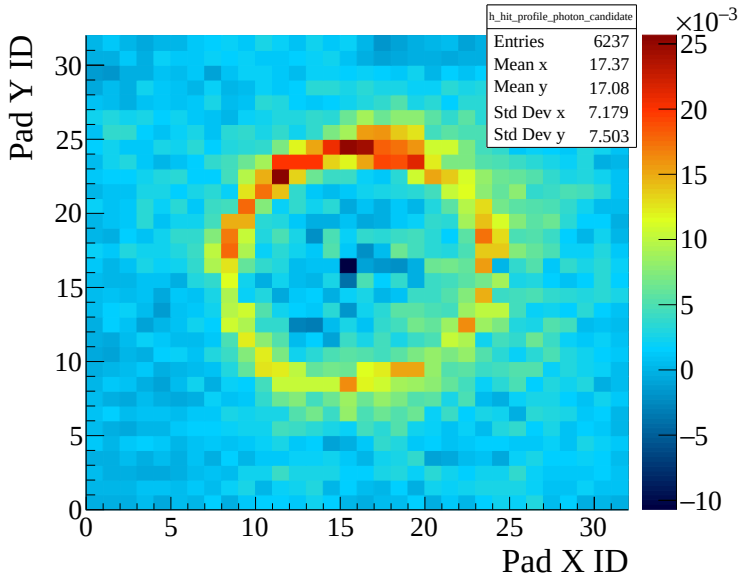

Figure 31: 2-D histogram of the difference between the 2-D histograms for events collected with the shutter between the radiator and the photocathode open and closed. The histogram population has been normalized with the ratio of the number of events in the two samples.

and ion bombardment. Moreover, CsI is chemically fragile: if exposed, even for short time, to atmospheres with water vapor, the molecule is broken and therefore the QE is lost. This feature imposes to assemble the photon detectors in clean, controlled atmospheres, making the overall detector construction tedious and complex. Therefore, the possibility of an alternative photocathode material adequate for gaseous detectors can represent a relevant step forward in the field of these sensors.

The Quantum Efficiency (QE) of photocathodes by NanoDiamond (ND) particles rich in graphite have been measured in vacuum [6]: when the photocathode is hydrogenized, QE as high as 47% at 140 nm has been measured; globally, the quantum efficiency is non-negligible in the VUV domain, below 210 nm. High QE-values have been measured both performing the hydrogen plasma treatment in situ, namely after coating the substrate with the photocathode film, and hydrogenated the ND powder before coating the substrate with the photoconverting layer. The latter option is of great interest for gaseous photon detectors: if fact, the hydrogen plasma treatment requires high temperature ($> 850\ ^oC$), not compatible with the components of gaseous detectors. When the ND powder is hydrogenated before the cathode coating, the spray procedure by an ultrasonic atomizer used to form the photocathode does not require temperatures exceeding 120 ^oC: this is compatible with gaseous detector components. Preliminary tests of mechanical attachment of the photocathode and aging due to exposure to air indicate that this photocathode material is robust.

Two principle difficulties must be considered in the context of the ongoing studies:

- The ND powder provided by the producers is a cheap material not selected according to the graphite content or the grain size; therefore, several different samples have to be purchased and then the graphite-rich ones have to be selected by Raman spectroscopy; no exact reproducibility of the raw material from producers can be envisaged at the moment;
- using the present set-up for the formation of photocathodes by the spray technique, the maximum photocathode size is of about 4 cm^2.

This activity has been ongoing since year 2018. A short summary of the exercises performed is listed in the following.

- In 2018 and in 2019, two series of small-size (3×3 cm^2) THGEMs have been coated with ND powder films, both hydrogenated and not hydrogenated; these electron multiplications have been characterized before and after applying the coating to comparatively access the effect of the photocathode on their performance as multipliers; after initial difficulties, an after-coating protocol has been established and the THGEM performance in terms of gain and stability is largely unmodified when coated.
- The effective Quantum Efficiency (QE) is a key parameter for the performance of gaseous photon detectors. The effective QE in gas has been measured by several groups and reproduced in simulation studies where the back scattering by the gas molecules is taken into account. We have started exercises to measure the effective QE in gasses of interest when HND photocathodes are used. When the measurement campaign is completed, we will verify if the back scattering by the gas molecules is adequate to describe the effective QE also for the novel photoconverter. The preliminary measurements indicate an evolution versus the electric field in front of the photocathode similar to that observed for CsI. This campaign of measurement has to be continued.
- The production of THGEMs formed by two layers, each one of thickness one half that of the final THGEM has been attempted. The goals was the possibility to coat one of the two surfaces using only a half THGEM, then combining the two parts in order to avoid coating inside the hole that can create shorts between the two THGEM face. The exercise was not successful.
- The effective QE versus the number of spray shots has been measured: it saturates at 50 spray shots.
- The exploration of the characteristics of the ND powder used as photo-converters is ongoing. The QE obtained using powders with different grain size has been measured. For small grain-size (a few nm) the QE is low. It increases with grain size up to sizes of about 50 nm. It does not increase further for larger grain-sizes.

B Appendix: SBU

The planned R&D effort for the SBU part is described herein.
Based on the Deliberation Document on the 2020 update of the European Strategy for Particle Physics it can be expected that in the foreseeable future the access to gasses with a high GWP, like fluorocarbons, is limited. It does not necessarily imply that such gasses will cease to exist, however, the commercial production could be in short supply such that the gasses could become prohibitively expensive. Standard fluorocarbons are making up the Cherenkov media for accessing high momentum particles because of their favorable characteristics. In order to be pro-active we are aiming to investigate the properties of noble gasses which have to be operated at rather high pressure for them to mimic the properties of fluorocarbons.
We are proposing the study of high pressure Ar-radiator based Cherenkov detectors. The index of refraction

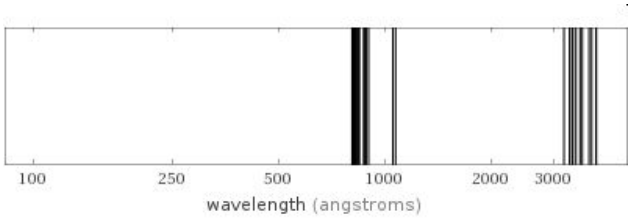

Figure 32: Atomic spectral lines for Argon I (neutral Argon) in the UV region.

for our previously used radiator CF_4 (in general wavelength dependent) has been $n_r(\lambda) - 1 \sim 5.5 \times 10^{-4}$ for λ=140 nm [7]. For achieving a similar index of refraction with Ar a simple relation can be used: $\eta = \eta_0 P/P_0$, with $\eta = n - 1$ and the subscript 0 indicates the quantity considered at atmospheric pressure. Consequently, the index of refraction for pressurized Ar can be made similar to CF_4 when using a pressure of about 1.5 atm [1]. The transparency is basically determined by the band-gap energy for Ar and it is quite favorable in the VUV range (see Fig. 32 [8]) for this radiator. The aim of this proposal is to replace the radiator CF_4 with Argon and perform similar studies as described in [9]. The replacement of the radiator implies that also the medium for the MPGD amplification stage is changed. Studies for operations of MPGD in pure Argon have been performed [10] and it has been shown that sufficiently high gains can be achieved in pressurized Argon for obtaining high photo-electron efficiency. Our R&D plan is three-fold:

(i) Reproduce and extend results from ref. [10].

(ii) Investigate photo-electron detection efficiency.

(iii) Investigate RICH performance with high-pressure Argon radiator.

For (i) we will operate our RICH prototype vessel under P = 1.5 atm and obtain the gain characteristics of a triple-/quadruple-/quintuple-GEM. Once the operation under high pressure is established we will continue to (ii) by producing a ring pattern of Al-dots on the surface of the top-GEM facing the radiator volume. The dot-pattern will be deposited with the e^--beam evaporation unit at SBU. Alternatively, we might want to acquire GEMs with a specialized pattern such the the Cr-layer is partly exposed in form of a ring. Chromium has a similar work function as Al. We will shine UV-light with known intensity onto the pattern for mimicking a Cherenkov ring and obtaining the photo-electron efficiency. Eventually, we are moving to step (iii) and will use the whole setup for obtaining the separation power for π-K and K-p.
An improvement for the separation power can be expected when using a readout pattern for the RICH that provides the ring construction. As shown in Fig. 33, a significant improvement for 3-σ separation can be achieved when using a readout pattern with a resolution of 500 μm. This would require to decrease the size of the pads on the readout board which in turn would increase the readout channel count. A promising solution to overcome this problem is to use the readout structure as described in Appendix D.2. We are aiming for replacing the hexagonal readout board that has been used in our previous test-beam campaign with the above mentioned board.

[1] $\eta_0 = 3.95 \times 10^{-4}$ for Ar.

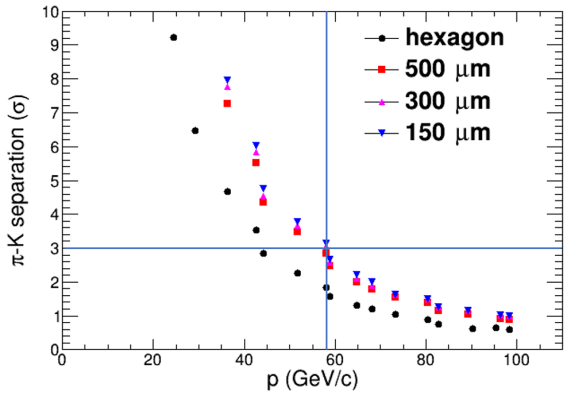

Figure 33: π-K separation power obtained with the RICH prototype [9]. The horizontal and vertical lines are for guiding the eye.

C Appendix: Temple U.

The angular resolution study (Sec. 4.2.2) carried out within the EicRoot framework included the following detectors and resolutions:

- Silicon Vertex Tracker
  - $5.8\mu \times 5.8\mu$ resolution
- TPC
  - Longitudinal intrinsic resolution: 500μ
  - Transverse intrinsic resolution: 90μ
  - Longitudinal dispersion: $1\mu/\sqrt{D[cm]}$
  - Transverse dispersion: $40\mu/\sqrt{D[cm]}$
  - Pad size: 1 cm
- Cylindrical μRWELL trackers
  - 100×100 resolution

D Appendix: UVa

D.1 Development of capacitive-sharing large-pad anode readout

We have been developing a new concept of pad readout PCB as anode readout for MPGD technologies that, by design combine the advantages of providing excellent spatial resolution performances i.e. better than 100 μm with large side pad greater than a few cm^2 and therefore considerably reducing the number of electronic channels required to readout large area MPGD detectors such as the ones under investigations for EIC various tracking systems. The basic principle is illustrated on the sketch of Fig. 34 and is based on vertical stack of square Cu-pad layers, separated by 50 μm thick kapton foils as dielectric to form a capacitor. The pad size doubles (and subsequently the area is multiplied by 4) from a one layer (layer layer[i]) to the layer[i+1] underneath it. Each pad of layer[i] is arranged is space so that its center is either always perfectly

Principe of **High-Resolution & Large-Pad** Anode Readout for MPGDs

5-Pad-Layers Configuration

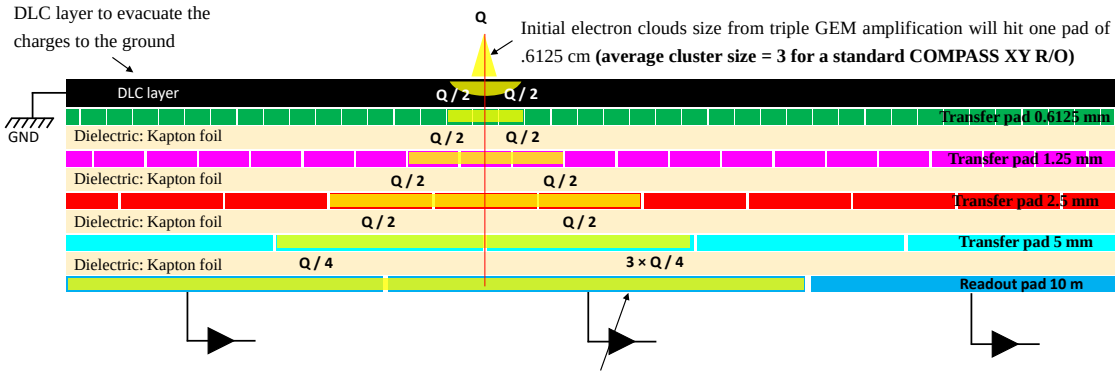

Figure 34: Principle of capacitive-coupling large-pads anode readout for MPGDs.

aligned with the center of a larger pad of layer[i+1] or with the boundary between of two adjacent pads of layer[i+1]. This space arrangement of the pads from one layer to the other ensured that the charges collected by two adjacent pads of layer[i] are always transferred to two adjacent pads of layer[i+1] no matter how the size of the pads of layer[i+1]. The charge are transferred between layers via capacitive coupling as two Cu-pad layers separated by the kapton foil acts effectively a perfect capacitor. The pads of the bottom layer[n], that we name here *charge-collection layer* are connected to the front end (FE) electronics readout, while all the other pad layers above, that we name here *charge transfer layers* just serve to transfer and spread the original charges through capacitive coupling. With such scheme the area a[n] of the pad of the *charge-collection layer* (layer[n]) in a n-layer-stack readout board is equal to a[1]$\times 2^n$ with a[1] being the area of the pad of the top *charge transfer layer* (layer[1]) and the total number of pads of layer[n] is $1/2^n$ of the total number of pads of layer[1]. By design, the top layer pad size of this readout board basically defines the spatial resolution performances of the pad readout scheme and in effect which is transferred via capacitive coupling the bottom layer which pad size define the total number of channel count to be read out.

With this scheme, in the first order, the spatial resolution performances is decoupled from the size of the readout layer pads connected to the FE readout electronics. So, for example, a 5-layers large-pad readout PCB with a pad size of 0.06125 cm $\times$ 0.06125 cm for the top layer will have a pad size equal to 1 cm $\times$ 1 cm for the bottom layer for the charge collection which will only require 100 channels to be read out in a standard 10 cm $\times$ 10 cm Triple-GEM detector configuration. This is **5 time less channels that the standard 2D X-Y COMPASS strips readout** which require 512 channels to achieve similar spatial resolution performance .

D.2 Applications of capacitive-sharing & large-pad readout for MPGDs:

Several other groups within eRD6 are interested in this large pad & high performance readout plane concept for various applications.

- **Large pad readout for Fast μRWELL layer in the barrel region:** This novel high performance large-pad readout concept is an extremely attractive option for the anode readout layer of the cylindrical μRWELL layer that we are investigating to perform as fast and precise tracking layer in the barrel region to complement the TPC central tracker and MAPS vertex detectors. As an example for the 60 cm $\times$ 60 cm cylindrical μRWELL prototype that we are proposing to build and characterize for the coming FY21 cycle, such a large-pad readout with a pad pitch 2 cm $\times$ 2 cm will require $\approx$ **900**

readout channels to read out the detector compared to $\approx$ **3000 channels** in the case of U-V strips readout configuration. This is our main motivation to pursue aggressively in this direction to optimize the parameters require to achieve the best performances for this novel type of pad readout.The newly joined eRD6 member group from Saclay are also interested in exploring the large-pad readout as anode readout option for the EIC full cylindrical micromegas trackers option.

- **Pad readout plane for GEM-RICH at Stony Brook:** The eRD6 colleagues at SBU are interested in testing the large-pad readout with the GEM-RICH prototype concept that they developed for high momentum hadron PID applications. The concept of the large-pad will allow significantly better space point resolution with lower readout channel count than the conventional hexagonal pad readout PCB board that is used for the current GEM-RICH prototype during the 2013 test beam. The pad size of this anode readout board and therefore the space point resolution performance became one of the identified limiting factor for reaching separation at higher momentum from that test beam data.

- **Large pad readout for EIC TPC GEM readout planes:** Another very interesting application is to couple the large-pad readout with the GEM amplification foils or any hybrid MPGD for EIC TPC end cap readout detectors. One such large-pad readout, with pitch size that is twice the pitch in both dimensions of zigzag readout layer used for the sPHENIX TPC GEM will reduce by 4 the number of electronic channels while providing a better space point resolution performances than the zigzag readout board. A reduction by 4 of the number of channel also means that number of SAMPA FE board needed at the back of GEM readout and the associated services required for cooling and power will be reduced by a factor 4. This is a huge benefice for EIC where reducing cost of the readout electronic as well as minimizing the material budget in the end cap region of the detector are both critically important. And considering the low particle rate expected in the EIC environment compared to sPHENIX, increasing the pad size is not expected to impact the performance of the detector.

D.3 Minimization of capacitance noise and cross yalk

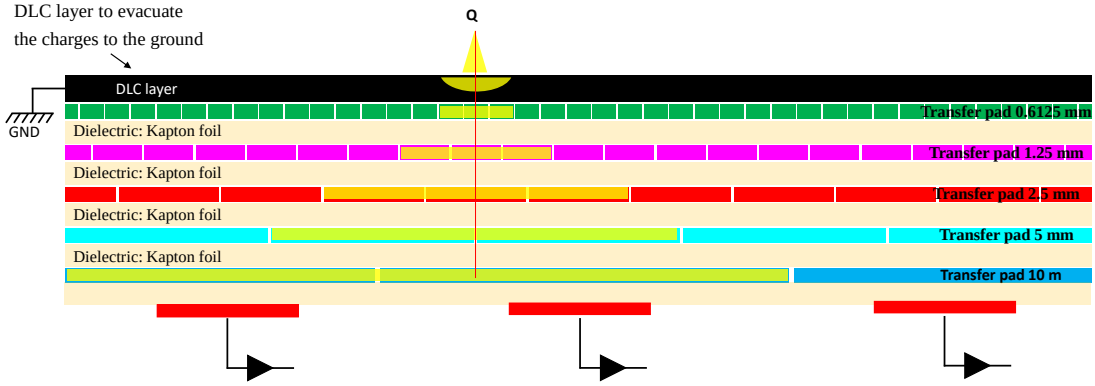

Figure 35: Sketch of a large-pad capacitive-coupling readout board with 4 quadrants, each with a different pad design to study the capacitance noise and cross talk effect.

We are also investigating ways to reduce the cross talk and capacitance noise induced by the large readout pads (inter-pad capacitance and cross talk) as well as between pads from different layers. This is crucial to maintain the spatial resolution performances as well as the efficiency of the detectors. The first study aims to address the inter-pad capacitance induced noise of the *charge-collection layer*. The idea is to add one additional pad layer to collect the signal but with smaller pads size as shown on the sketch of Fig. 35. This scheme will significantly decrease the inter-pad capacitance noise and cross talk between pads while we maintain the charge sharing capabilities therefore the spatial resolution performances. However the amplitude of the signal collected by the FE pre-amplifier will be significantly smaller, however we could

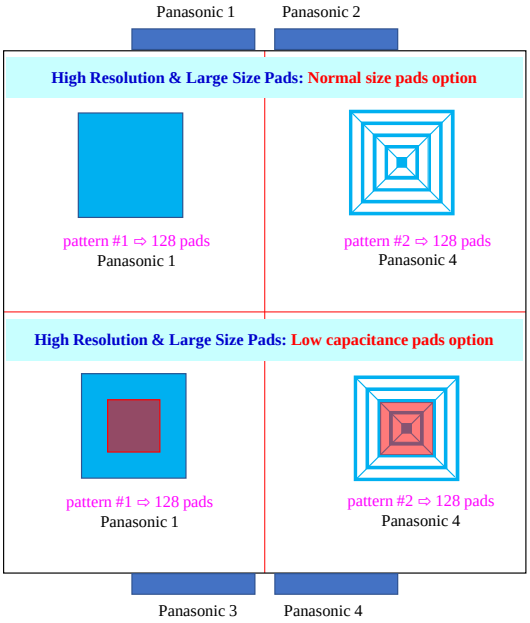

Figure 36: Sketch of a large-pad capacitive-coupling readout board with 4 quadrants, each with a different pad design to study the capacitance noise and cross talk effect.

easily compensate the signal to noise ratio by increasing the gain of the detector by increasing the GEM or μRWELL amplification gain. Another area is to actually study various pad design as shown on the right side of the cartoon of Fig. 36 with the spiral like square pad pattern to reduce the area of the large pads. This will help further with both cross talk and capacitance noise reduction.
We plan to test on a single readout board 4 patterns with same pad pitch in 4 quadrants of the active area. the top left will be the standard readout large plain Cu-pad, the bottom will have the plain Cu pad but signal collected by the smaller pad size as descried on Fig. 35. On the top right, we will look at spiral pad design and on bottom right the same spiral pad but with smaller collection pad for the FE electronics.
The study of these four designs in a single readout board will allow us to perform a one-to-one comparison of the impact of the pad design both on the capacitance noise and cross talk performances to optimize the the signal to noise ratio which is a crucial parameter for achieving the requirements in term of spatial resolution and detector efficiency. In the second step of the study, we plan to propagate the select optimized pad pattern to the other *charge transfer layers* and perform a more comprehensive study of the overall impact on noise and cross talk improvement but also more importantly to help reducing the material thickness of the readout board.